European Journal of Cell Biology 102 (2023) 151334

Contents lists available at ScienceDirect

European Journal of Cell Biology

journal homepage: www.elsevier.com/locate/ejcb

Bone marrow mesenchymal/fibroblastic stromal cells induce a distinctive EMT-like phenotype in AML cells

N. Nojszewska [a,1], O. Idilli [a,1], D. Sarkar [a,1], Z. Ahouiyek [a,1], Y. Arroyo-Berdugo [a], C. Sandoval [b], MS Amin-Anjum [a], S. Bowers [a], D. Greaves [a], L. Saeed [a], M. Khan [a], S. Salti [a], S. Al-Shami [a], H. Topoglu [a], JK Punzalan [a], JG Farias [b], Y. Calle [a,*]

[a] School of Life and Health Sciences, University of Roehampton, London SW15 4JD, UK
[b] Department of Chemical Engineering, Universidad de La Frontera, Temuco, Chile

ARTICLE INFO

Keywords:
AML
Tumour microenvironment
EMT
Migration
Vimentin
F-actin
Cell adhesion

ABSTRACT

The development of epithelial-to-mesenchymal transition (EMT) like features is emerging as a critical factor involved in the pathogenesis of acute myeloid leukaemia (AML). However, the extracellular signals and the signalling pathways in AML that may regulate EMT remain largely unstudied. We found that the bone marrow (BM) mesenchymal/fibroblastic cell line HS5 induces an EMT-like migratory phenotype in AML cells. AML cells underwent a strong increase of vimentin (VIM) levels that was not mirrored to the same extent by changes of expression of the other EMT core proteins SNAI1 and SNAI2. We validated these particular pattern of co-expression of core-EMT markers in AML cells by performing an *in silico* analysis using datasets of human tumours. Our data showed that in AML the expression levels of *VIM* does not completely correlate with the co-expression of core EMT markers observed in epithelial tumours. We also found that *vs* epithelial tumours, AML cells display a distinct patterns of co-expression of *VIM* and the actin binding and adhesion regulatory proteins that regulate F-actin dynamics and integrin-mediated adhesions involved in the invasive migration in cells undergoing EMT. We conclude that the BM stroma induces an EMT related pattern of migration in AML cells in a process involving a distinctive regulation of EMT markers and of regulators of cell adhesion and actin dynamics that should be further investigated. Understanding the tumour specific signalling pathways associated with the EMT process may contribute to the development of new tailored therapies for AML as well as in different types of cancers.

1. Materials and methods

1.1. Cell culture

The Human AML cell lines eGFP-MOLM14 and eGFP-MV4–11 and the BM stromal cells HS5 and mCherry-HS5 were previously generated using lentiviral vectors (Arroyo-Berdugo et al., 2023). Cell lines were cultured at 37 °C in a humidified atmosphere in the presence of 5 % CO_2, 95 % air. eGFP-MOLM14 cells were cultured in RPMI-1640 medium and mCherry-HS5 cells in DMEM supplemented with L-glutamax, both supplemented with 10 % foetal bovine serum (FBS).

1.2. Image acquisition and analysis

mCherry-HS5 BM fibroblastic stromal cells were seeded at 10×10^3 cells/per well in 96 well plates in DMEM supplemented with 10 % FBS. The following day, the culture media was aspirated and eGFP-MOLM-14 cells were layered on mCherry-HS5 cells at a density of 2×10^5 cells/ml in 200 µl per well of RPMI supplemented with 10 % FBS. Three technical replicas were seeded per experimental condition. At day 3, cultures were filmed using time-lapse video by capturing micrographs of the eGFP (λex488nm/λem528nm), mCherry (λex584nm/λem607nm) every minute for 20 min and phase contrast channels using the 10X lens and 1.5X magnifier of a Nikon Elipse Ti microscope. Avi files of the eGFP channel were exported and analysed using the Trackmate plugin in FIJI (https://

* Corresponding author.
E-mail address: yolanda.calle-patino@roehampton.ac.uk (Y. Calle).
[1] These authors contributed equally.

https://doi.org/10.1016/j.ejcb.2023.151334
Received 6 February 2023; Received in revised form 14 June 2023; Accepted 15 June 2023
Available online 17 June 2023

imagej.net/software/fiji/) to determine the velocity and displacement of cells. Single micrographs were used for quantification of the percentage of elongated cells. A lattice of nine square regions was placed per field of view and the number of elongated and total cell per square in the field was determined using the counting tool of FIJI. Still micrographs from the same films were analysed to determine de grade of circularity of cell shape using FIJI. Circularity values range from 0 (infinitely elongated shape) to 1 (perfect circle).

1.3. Immunofluorescence

Freshly prepared 10 μg/ml bovine fibronectin (Sigma) solution was incubated over sterile glass coverslips for 1 h at room temperature before plating eGFP-MOLM14 and HS5 cells as described above for the live imaging experiments. At day 3, eGFP-MOLM14 cultured alone or in the presence of HS5 cells were fixed with 4 % PFA/3 % sucrose for 25 min and permeabilised with 0.05 % Triton-X-100/PBS for 10 min. Localization of VIM was achieved by means of incubation with an anti-VIM antibody (SigmaAldrich, cat No V6630) diluted 1:500 in 2.5 % BSA/PBS at room temperature for 1 h. After three PBS washes, samples were incubated with an Alexa568-tagged anti-mouse secondary antibody diluted in 2.5 % BSA/PBS for 45 min at room temperature. Coverslips were then washed three times with PBS and twice with distilled water before being mounted in Vectashield mounting medium (Vector Laboratories, UK). Fluorescence images were captured with a Nikon Elipse Ti microscope using the NIS-Elements was used for collection and storage. Images were exported as TIFF files and processed with Adobe Photoshop 2023 software.

1.4. Zymography

mCherry-HS5 BM cells were seeded at 10^5 cells/per well in 6 well plates in DMEM supplemented with 10 % FBS. The following day, the culture media was aspirated and eGFP-MOLM-14 cells seeded at a density of 2×10^5 cells/ml in 4 ml l per well of RPMI supplemented with 10 % FBS. At day 3 of culture, the culture medium was replaced with RPMI and cells were incubated for 48 h. The supernatants were collected, centrifuged (900 g for 5 min) to remove cells debris and mixed with non-reducing Laemly buffer and subjected to sodium dodecylsulfate-polyacrylamide gel electrophoresis(SDS-PAGE) in 0.75 mm,10 %(w/v) acrylamide gels containing 0.075 % (w/v) gelatin at 4ºC. Gels were soaked in 2.5 %(v/v)Triton X-100 with gentle agitation at room temperature for 30 min to remove the SDS from the gels and to allow protein renaturation. Gels were rinsed once with substrate buffer (0.05MTris–HCl, pH8' 0;1 mM CaCl2) and incubated in fresh substrate buffer at 37 ∘C overnight. Then, gels were stained with Coomassie blue stain under shaking for 30 min, followed by de-staining in distilled water until suitable visualisation of digested gelatin bands was achieved. Gels were imaged using the ChemiDoc from Biorad. Quantification of area and pixels intensity of formed bands was determined using the analysis tools of Adobe Photoshop 2023 to calculate the integrated intensity values by multiplying the values of the two parameters. All experiments were repeated 3 times.

1.5. Western blot

Approximately 20 μg of total cell lysate protein in Laemly buffer were loaded per lane in a 12 % SDS-PAGE gel and subjected to electrophoresis. Proteins were blotted onto nitrocellulose membranes with a Bio-Rad Mini protein II transfer apparatus. Membranes were blocked with 5 % dried milk/TBS-T for 1 h at room temperature, incubated with antibodies against the proteins of interest at the concentrations indicated by the suppliers at 4 C overnight with gentle agitation. After three washes with PBS-T, immunoprobed proteins were detected by incubation with horseradish peroxidase-conjugated secondary antibodies at room temperature for 1 h. After further washes in PBS-T, immunoprobed proteins were visualized by immunofluorescence or ECL chemiluminescence kit (Amersham, UK) and the signal emitted was collected using a Li-cor Odyssey XF® imaging system.

1.6. In silico analysis of the correlation between the expression of VIM and genes of interest

The potential co-expression of *VIM* and groups of proteins of interest (core EMT markers, actin polymerisation regulators and actin-binding proteins, proteins involved in podosome and invadopodia formation) was performed using the bioinformatics tool cBioportal analysis suite (Cerami et al., 2012; Gao et al., 2013). Pearsonś and Spearman's values (R) for linear and monotonic correlations were determined for each *VIM* /gene of interest pair in each tumour type analysed. Significant co-expression correlation values ($p < 0.05$) were considered according to the correlation coefficient as weak (0.20–0.39), moderate (0.40–0.59), strong (0.60–0.79) or very strong (0.80–1.0).

1.7. Statistics

For statistical analysis using the adequate tests, GraphPad Prism 9 software was used. Statistically significant difference using Mann-Whitney was determined from $p < 0.05$.

2. Introduction

Epithelial Mesenchymal Transition (EMT) was first defined as a process in which epithelial cells disassemble the stationary attachments to the surrounding tissue and acquire a migratory phenotype, correlating with the downregulation of molecular epithelial markers and the acquisition of mesenchymal morphological and molecular features. This process is key for tissue remodelling during embryonic development and wound healing (Yang et al., 2020). The development of the EMT phenotype involves at the molecular level the expression of a series of transcription factors that include SNAIL/SNAI1, SLUG/SNAI2, TWIST and the ZEB family of transcription factors, which in turn downregulate the expression of E-cadherin (Thiery and Sleeman, 2006) and upregulate and activate N-cadherin and the intermediate filament vimentin (VIM) (Meng et al., 2018). The expression and organisation of VIM filaments facilitate the migratory and invasive phenotype of cells that undergo EMT.

The expression of EMT markers is also associated with aggressive forms of cancers and poor prognosis of patients (Kahlert et al., 2017; Pastushenko and Blanpain, 2019; Stavropoulou et al., 2016; Yang et al., 2020). EMT is thought to play a key role in tumour progression by facilitating an invasive phenotype in cancer cells that enables dissemination and metastasis (Pastushenko and Blanpain, 2019). Cancer cells bearing an EMT phenotype also exhibit additional malignant characteristics such as cancer stem cell properties (Guo et al., 2012), immunosuppressive capacity (Noman et al., 2017; Terry et al., 2017) and resistance to radiotherapy (Galeaz et al., 2021; Yu et al., 2021) and drug treatments (Zhang et al., 2021a; Zhang et al., 2021b). Although the development of an EMT phenotype was initially described in tumour of epithelial origin (carcinomas), it was later revealed that cancers of mesenchymal origin including both solid tumours and haematological malignancies also undergo EMT-like processes (Kahlert et al., 2017; Yang et al., 2020). In multiple myeloma (Azab et al., 2012; Cheong et al., 2020; Ibraheem et al., 2019) and in Acute Myeloid Leukaemia (AML) high levels of expression of EMT markers has been shown to correlate with increased motility (Kahlert et al., 2017; Stavropoulou et al., 2016), tumour progression and/or poor prognosis in patients (Kahlert et al., 2017; Stavropoulou et al., 2016).

It is well documented that in solid tumours, various factors in the tumour microenvironment (TME) including hypoxia (Choi et al., 2017; Lin et al., 2016) and secretion of cytokines, growth factors (Ramundo et al., 2021) and extracellular matrix proteins (Dai et al., 2019; Fattet

et al., 2020) by cellular components such as cancer associated fibroblasts (CAFs) (Attieh and Vignjevic, 2016) provide chemical and mechanical cues that can induce an invasive migratory EMT phenotype in cancer cells. The crosstalk between cancer cells and the TME can shape the overall tumour organisation and the extent of development of the EMT phenotype in cancer cells (Ligorio et al., 2019) and as a result, the prognosis and response to therapy (Fiori et al., 2019; Wang et al., 2018). The role of the TME in modulating EMT is not as well characterised in haematological malignancies (Greaves and Calle, 2022). Multiple myeloma is the haematological tumour where the regulation of EMT by the TME has been studied in more depth. There is compelling evidence that multiple myeloma cells can undergo an EMT process in response to hypoxia (Azab et al., 2012) that results in increased migratory potential and dissemination of cells to new sites in the bone marrow (BM) (Azab et al., 2012; Cheong et al., 2020; Ghobrial, 2012; Ibraheem et al., 2019). It has also been shown that BM mesenchymal/fibroblastic stromal cells can secrete extracellular matrix proteins that promote EMT in myeloma cells (Ibraheem et al., 2019). Taken together, the results in myeloma raise the possibility that the TME may induce a migratory EMT phenotype in other haematological malignancies contributing to disease progression and response to treatments. The TME factors that may induce EMT and the exact pattern of the regulation of EMT markers in AML and in other haematological malignancies remain largely unknown.

The enhanced migratory capacity of cells that undergo EMT is the result of the remodelling of their cytoskeletal networks and cell adhesions (Greaves and Calle, 2022). Invadopodia are F-actin based structures containing VIM filaments, which have been described as key structures that facilitate the invasive migration of cancer cells during EMT (Linder et al., 2023). Podosomes are related structures to invadopodia that belong to the same family of invasive adhesions called invadosomes. Formation and turnover of these adhesions are regulated by the dynamic polymerisation of F-actin, which is controlled by actin-binding proteins. These include the actin nucleating factor Arp2/3 complex and its activators, the nucleators binding proteins of the WASP/WAVE family and F-actin bundling proteins such as fascin and α-actinin. Cell adhesion molecules of the integrin family and associated intracellular proteins are structural and also regulatory components of invadopodia and focal contacts formed by invasive cancer cells (Greaves and Calle, 2022). The specific expression levels and organisation of these proteins in adhesive signalling platforms in different types of cancers regulate their particular pattern of migration, as well as other critical aspects of carcinogenesis such as immunosuppression and drug resistance (Biber et al., 2021; Greaves and Calle, 2022; Izdebska et al., 2020). The defined co-expression of EMT markers with the components of adhesions and the cytoskeleton in different cancers may explain the tumour type-associated patterns of tissue localisation and response to treatments.

In the current study, we show that BM mesenchymal/fibroblastic stromal cells induce a migratory phenotype in AML cells that correlates with a distinct pattern of co-expression of VIM with SLUG and SNAIL divergent from the classical co-upregulation of these EMT markers in epithelial tumours. We performed an *in silico* analysis of the transcriptome of human tumours and validated our *in vitro* results. Our data showed that AML cells display low or no correlation between the expression levels of *V IM* and the EMT markers *SNAI1/2, ZEB1/2 and TWIST1/2*, a feature that was shared with solid tumours of mesenchymal origin. In contrast, epithelial tumours show a strong correlation between the expression of VIM and classical EMT transcription factors. We also investigate the possible correlation between the expression of *V IM* and the cytoskeletal and integrin-related proteins that are present in the adhesions formed by cancer cells undergoing EMT (Greaves and Calle, 2022) and compare the patterns in AML *vs* solid tumours. We studied the possible role of BM mesenchymal/fibroblastic cells in the regulation of the patterns of co-expression of *V IM* and some critical regulators of actin and cell adhesion dynamics identified *in silico* in AML tumours.

3. Results

3.1. BM mesenchymal/stromal cells induce an EMT migratory phenotype in AML cells

In order to investigate the impact of BM mesenchymal/fibroblastic cells on AML motility, we compared the activity of AML cell lines cultured alone *vs* in co-culture with the cytoprotective BM stromal cell line HS5. We used our experimental model based on the constitutive expression of fluorescent proteins (eGFP in AML cells and mCherry in HS5 cells), which allows to easily distinguish the two cell populations in co-culture (Arroyo-Berdugo et al., 2023). AML cells cultured alone displayed a circular morphology with a smooth surface (Fig. 1 A-B). In contrast, in the presence of mCherry-HS5 cells, AML cells commonly displayed a more irregular surface due to the development of membrane extensions (Fig. 1 D-F) correlating with a significant increase in the presence of elongated cells (Fig. 1 G) and an overall decrease in circularity (Fig. 1 H). These changes in morphology reflected the enhanced membrane protrusive activity and increase in cell velocity and displacement of AML cells in co-culture with mCherry-HS5 cells (Fig. 1 I-L; Supplementary videos 1–4).

Migration of AML cells and extramedullary infiltration of AML blasts has been linked to the secretion and/or expression of matrix degradation and remodelling enzymes such as elastases (Tavor et al., 2005) and the metalloproteinases (MMPs) MMP-2 and MMP-9 (Chaudhary et al., 2016; Pirillo et al., 2022; Sawicki et al., 1998; Zhang et al., 2004). MMPs are involved in the invasive migration of AML cells by facilitating tissue remodelling and vessel leakage resulting in the release from the BM into the blood system (Pirillo et al., 2022). Accordingly, we detected the secretion of MMP-2 (pro-active and/or active forms) and MMP-9 in its proactive form in the supernatants from co-cultures of AML cells (eGFP-MV4–11 and eGFP-MOLM14) with mCherry-HS5 cells (Fig. 2 A-C). In contrast, AML cells cultured alone secreted very low amounts of pro-active MMP-9 (eGFP-MV4–11 cells) or undetectable levels of MMPs (eGFP-MOLM-14). mCherry-HS5 cells cultured alone secreted the pro-active form MMP-2 at similar levels as detected in co-culture with the two AML cell lines tested, whereas lower levels of active MMP-2 were detected in monoculture in comparison to secretion in co-culture with eGFP-MV4–11 cells. Taken together, our results show that in co-culture with BM stromal cells, AML cells develop a migratory phenotype linked to the secretion of MMP-2 by BM mesenchymal/fibroblastic cells and the increased secretion of MMP-9 by AML cells into the surrounding medium.

Secretion of MMPs is characteristic of cells undergoing mesenchymal mode of migration and the significant expression of various classical EMT markers has been shown to correlate with enhanced motility of AML cells (Kahlert et al., 2017; Stavropoulou et al., 2016). We then investigated whether the observed migration of AML cells induced by the presence of BM stromal cells was associated with the development of an EMT-like phenotype. VIM was barely expressed in eGFP-MOLM-14 or eGFP-MV4–11 cells cultured alone (Fig. 2 D). However, in co-culture with BM stromal cells, AML cells exhibited a highly significant upregulation of VIM levels (19.6-fold and 11.4-fold increase in eGFP-MOLM-14 and eGFP-MV4–11 cells, respectively) (Fig. 2 D, E). Similarly to the pattern of co-expression described in epithelial tumours undergoing complete EMT, the observed increase in VIM levels correlated with a steep downregulation of E-cadherin (Fig. 2 D, F) and upregulation of N-Cadherin (Fig. 2 D, E) in AML cells in co-culture. The switch to the expression of VIM is critical to enable the migratory phenotype of cells undergoing EMT. AML cells in co-culture with BM-mesenchymal/fibroblastic stromal cells became more adhesive (Fig. 2 G) and displayed a localisation of VIM filaments at the cell margin or in the cytoplasm (Fig. 2 H) whereas AML cells cultured alone displayed a round morphology and were mostly devoid of VIM (Fig. 2 H).

In contrast, the mesenchymal markers SNAI1 (also known as SNAIL)

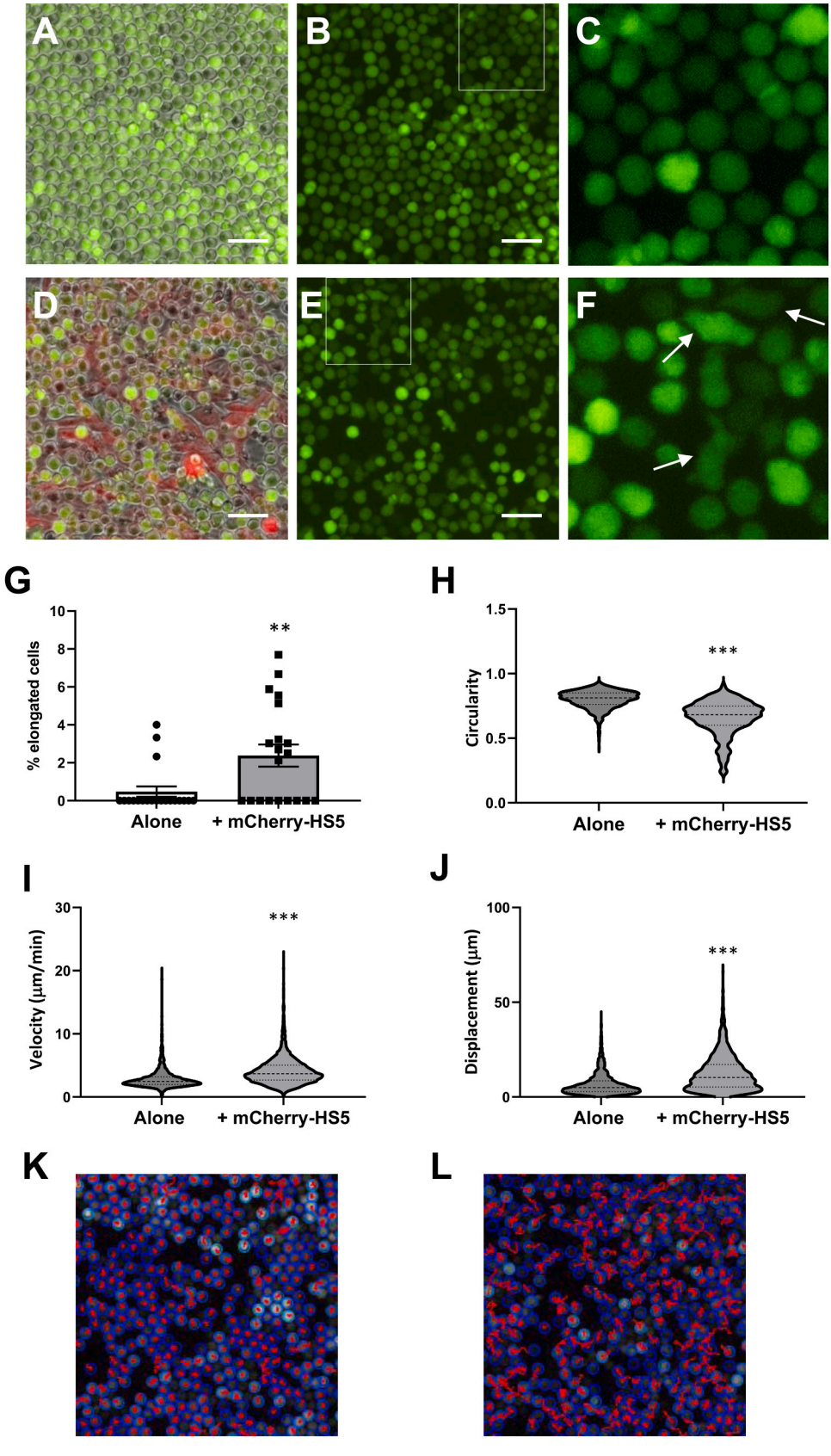

Fig. 1. BM mesenchymal/fibroblastic cells induce the migration of AML cells. Micrographs showing lives still images of eGFP-MOLM14 cells cultured alone (A-B) or in co-culture with mCherry-HS5 cells (D-F); Micrographs A and D show a composite of phase contrast and fluorescence images including the channel to detect mCherry (red) in mCherry-HS5 cells, B and E show the eGFP fluorescence image (green) showing the distribution of GFP-MOLM14 cells. Magnifications of the boxed areas in B ad E are shown in C and F, respectively. White arrows point at fully elongated eGFP-MOLM-14 cells. Bar 50 µM; (G) Graph showing the average and SD of the percentage of elongated eGFP-MOLM14 cells cultured alone or in the presence of mCherry-HS5 cells (+mCherry-HS5); (H) Graph showing the circularity index of eGFP-MOLM-14 as calculated using FIJI software; Graphs showing the distribution of the velocity (I) and displacement (J) values of eGFP-MOLM14 cells. * * $p < 0.01$; * ** $p < 0.005$ Man-Whitney test; (K, L) representative images showing the migration tracks of eGFP-MOLM-14 seeded alone and in the presence of mCherry-HS5 cells, respectively. Images were generated using the plugin Trackmate in FIJI and show only the tracks of cells detected the whole duration of the film.

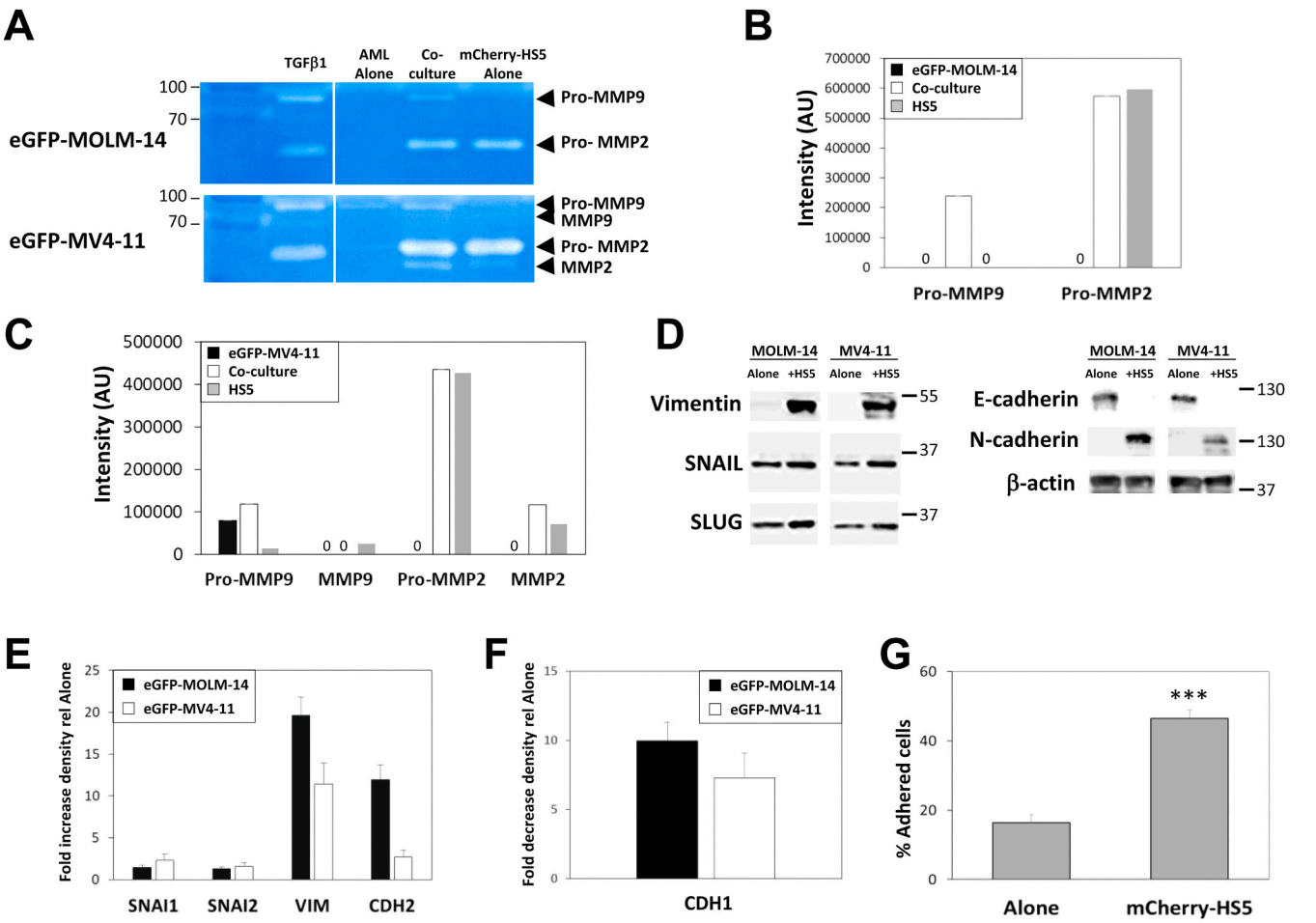

(caption on next page)

Fig. 2. BM mesenchymal/fibroblastic cells induce an EMT-like phenotype in AML cells. (A) Zymographies of supernatants collected from cultures of eGFP-MOLM14 or eGFP-MV4–11 cells. AML cells were cultured alone, cultured alone or AML and mCherry-HS5 cells in co-culture in RPMI supplemented with 10 % FCS for 3 days. Supernatants of AML cells incubated with 1 ng/ml TGFβ1 w ere used as positive control for MMP2 and MMP9 production by AML cells; (B, C) Quantification of the intensity of the bands detected in the zymographies measured in arbitrary units (AU); (D) Western blot analysis showing the levels of expression of VIM, SNAIL, SLUG, E-cadherin and N-cadherin in eGFP-MOLM14 and eGFP-MV4–11 cultured alone or in the presence of mCherry-HS5 cells (+HS5). Protein levels of β-actin were used as loading control; (E) Graph showing the average and SD of the relative value of the increase in the intensity of the bands of SNAIL (SNAI1), SLUG (SNAI2), vimentin (VIM) and N-Cadherin (CDH2) from samples obtained from AML and mCherry-HS5 cells in co-culture with respect to the values obtained from AML cells cultured alone (n = 3); (F) Graph showing the average and SD of the relative value of the decrease in the intensity of the E-cadherin (CDH1) bands from samples obtained from AML and mCherry-HS5 cells in co-culture with respect to the values obtained from AML cells cultured alone (n = 3); (G) Graphs showing the average and SD values of the percentage of adherent eGFP-MOLM-14 cells cultured alone or in the presence of mCherry-HS5 cells; (H) Micrographs showing eGFP-MOLM14 cells cultured alone (top panels) or in the presence of HS5 cells (middle and bottom panels). Images illustrate the distribution of VIM filaments (red) detected by immunostaining on eGFP-MOLM14 cells (green). Magnifications of the boxed areas are shown on the right of the micrographs. Arrow heads point at the localisation of VIM filaments at the cell margin of eGFP-MOLM14 cells.

and SNAI2 (also known as SLUG) were already expressed in AML cells at basal level and the upregulation in the levels of SNAI1 and SNAI2 induced by the presence of mCherry-HS5 cells was modest in comparison to the upregulation of VIM, ranging from 1.3 to 2.2-fold increase (Fig. 2 D, E).

Overall, we found that the presence of BM stromal cells promotes an EMT-like migratory phenotype in AML cells. Our data indicate that in this EMT-like process observed in AML cells show some similarities but also differs in the patterns of co-expression of classical EMT markers in comparison to classical EMT in epithelial tumours.

3.2. AML cells present a distinct pattern of co-expression of VIM and core EMT markers that differs from epithelial tumours

EMT was initially thought as a binary process where tumour cells displayed either a stationary epithelial or a migratory mesenchymal phenotype linked to the particular pattern of co-upregulation or repression of the EMT molecular markers. However, it is now well accepted that mesenchymal tumours, including AML can also undergo EMT-like processes that increase their migration capacity (Yang et al., 2020). The exact dynamics of the co-expression of EMT markers in AML cells during these EMT-like processes remain largely unknown.

Our data above indicate that the presence of BM stromal cells induce an EMT-related migratory phenotype with a distinct lack of correlation in the variations in the levels of SNAI1 and SNAI2 in relation to VIM or N-cadherin, which are significantly co-upregulated in comparison. In order to validate our *in vitro* findings and compare the dynamics of co-expression of EMT markers in AML *vs* epithelial cancers, we performed an *in silico* analysis of the pattern of co-expression of the mRNA transcripts of *VIM* and classical EMT markers in human tumours. We used the levels of *VIM* as an anchor for comparison of the co-expression of other EMT-related markers in our study because according to the latest guidelines by the EMT International Association, EMT is typically defined by a switch in intermediate filament usage to VIM whereas variation on the expression of the other EMT markers may not be as prominent and may vary in cells undergoing EMT according the type of cancer or the subpopulations within the same tumour (Yang et al., 2020). Additionally, VIM filaments are critical for enabling the enhanced migration of cells undergoing EMT (Yang et al., 2020).

Correlation analyses were performed using publicly available mRNA expression datasets from AML, epithelial (pancreatic, colorectal, breast and prostate carcinomas) and mesenchymal tumours (melanoma, lymphoid leukaemia and lymphoma) available in the cBioportal database and summarised in Table 1.

We considered relevant significant correlations of co-expression with *VIM* ($p \leq 0.05$) with Pearsońs correlation indexes $R > 0.2$ or $R < -0.2$ (Fig. 3). The initial characterisation of the EMT process described a downregulation of *CDH1* (E-cadherin) in parallel with an upregulation of *CDH2* (N-cadherin) and *VIM* (Yang et al., 2020). Our data show that all epithelial and AML tumours showed a significant inverse correlation between the levels of expression of *VIM* and *CDH1*, as expected based in the classical EMT model (Fig. 3A) and correlating with our results in the co-cultures of AML cells with BM mesenchymal/fibroblastic stromal cells (Fig. 2 D). The expected positive co-expression pattern between *VIM* and *CDH2* was observed in all the epithelial tumours and in the AML (OHSU, Nature 2018) database (Fig. 3 B), which correlated with our *in vitro* results (Fig. 2 D). However, all the others AML data sets showed a

Table 1
Summary of the datasets used for the correlation analysis, classified according to type of cancer. List of the study reference as listed in cBioportal (https://www.cbioportal.org/), cohort size and publication associated with the dataset of the datasets used to determine the co-expression of *VIM* levels with EMT markers and proteins associated with the molecular composition of invasive adhesions.

Cancer Type	cBioportal study reference	Cohort size	Reference
AML	Acute Myeloid Leukemia (TCGA, PanCancer Atlas)	173	(Liu et al., 2018)
Pancreatic adenocarcinoma	AML (TCGA, Firehose Legacy)	173	
	AML (TCGA, NEJM 2013)	173	(Cancer Genome Atlas Research, N. et al., 2013)
	Acute Myeloid Leukemia (OHSU, Nature 2018)	451	(Tyner et al., 2018)
	Pediatric Acute Myeloid Leukemia (TARGET, 2018)	45	
	Pancreatic Adenocarcinoma (QCMG, Nature 2016)	96	(Bailey et al., 2016)
	Pancreatic Adenocarcinoma (TCGA, Firehose Legacy)	179	
	Pancreatic Adenocarcinoma (TCGA, PanCancer Atlas)	177	(Liu et al., 2018)
Colorectal adenocarcinoma	Colorectal adenocarcinoma (TCGA, Firehose Legacy)	382	
	Colorectal adenocarcinoma (TCGA, Nature 2012)	244	(Cancer Genome Atlas, 2012)
Breast carcinoma	Breast Invasive Carcinoma (TCGA, PanCancer Atlas)	1082	(Liu et al., 2018)
Prostate cancer	Metastatic Prostate Cancer (SU2C/PCF Dream Team, Cell 2015)	118	(Robinson et al., 2015)
	Prostate Adenocarcinoma (TCGA, PanCancer Atlas)	493	(Liu et al., 2018)
Mesenchymal tumours	Pediatric Acute Lymphoid Leukemia - Phase II (TARGET, 2018)	203	
	Melanoma (MSK, NEJM 2014)	21	(Snyder et al., 2014)
	Diffuse Large B-Cell Lymphoma (TCGA, CanCancer Atlas)	48	(Liu et al., 2018)

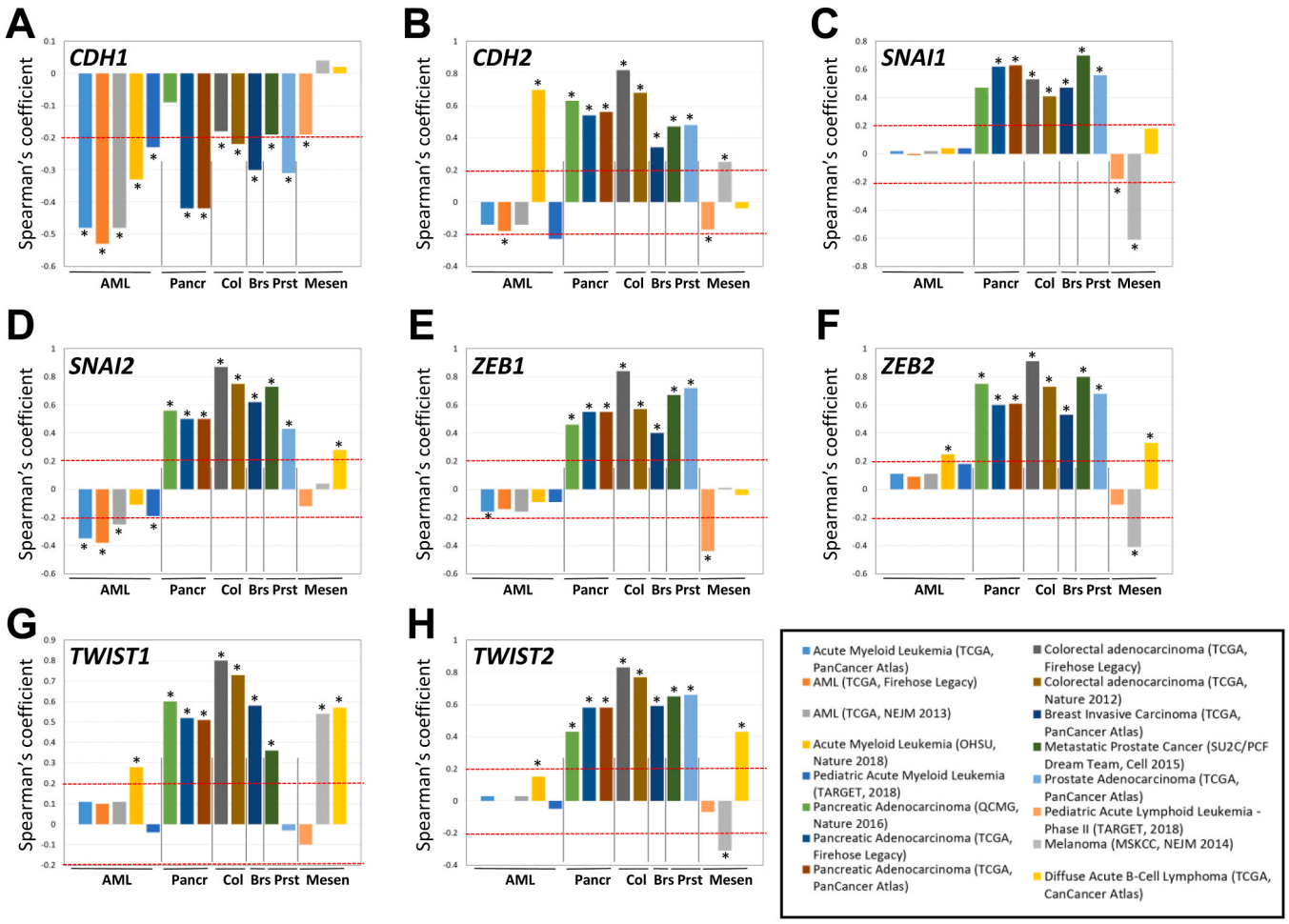

Fig. 3. Correlation between the mRNA expression of the *VIM* and core-EMT markers. Graphs showing the Spearman's coefficient correlation values between the co-expression of *VIM* with (A) *CDH1*, (B) *CDH2*, (C) *SNAI1*, (D) *SNAI2*, (E) *ZEB1*, (F) *ZEB2*, (G) *TWIST1*, (H) *TWIST2* obtained with the bioinformatics tools in cBioportal using datasets specified in the graphs legend obtained from human cancer tumours of Acute Myeloid Leukaemia (AML), pancreatic carcinomas (Pancr), colorectal cancers (Col), breast (Brs), prostate (Prst) carcinomas and mesenchymal cancers (Mesen). * $p < 0.05$ correlation statistical significance. The red dash lines show the coefficient values of − 0.2 and 0.2. The correlation values between − 0.2 and 0.2 were considered too weak to reflect significant co-expressions.

tendency to an inverse co-expression of *VIM* and *CDH2* whereas mesenchymal tumours did not display any consistent correlation. There was a clear pattern of co-expression of *VIM* and the core EMT markers studied (*SNAI1/2, ZEB1/2, TWIST 1/2*) consistently across all the epithelial tumours (Fig. 3 C-H) as it would be expected in classical EMT. As detected in our *in vitro* essay, in AML tumours there was no correlation between the variation in *VIM* levels and *SNAI1* (Fig. 3C) while a weak inverse correlation was detected with *SNAI2* levels (Fig. 3 D). Lack of significant co-expression was also detected between *VIM* and *ZEB1/2, TWIST 1/2* in AML tumours (Fig. 3 E-H). This pattern in AML was similar to that of the mesenchymal tumours studied.

Overall, our *in silico* data show a distinctive pattern of co-expression of *VIM* and some classical EMT markers in AML cells in comparison to epithelial tumours. These *in silico* results validate our data of the pattern of co-expression of VIM, CDH1, CDH2, SNAIL and SLUG in AML cells undergoing EMT induced by BM stromal cells.

3.3. Distinct pattern of co-expression of VIM and cytoskeletal components involved in EMT in AML in comparison to epithelial tumours

As a result of EMT, cancer cells acquire a migratory phenotype that requires major coordinated changes in cytoskeletal organisation. Nestin is another intermediate filament protein upregulated during EMT (Ishiwata, 2016; Zhang et al., 2016), which has been shown to regulate the dynamics of VIM filaments (Wang et al., 2022). Additionally, in parallel to the upregulation and polymerisation of VIM during EMT, cells undergo major rearrangements of F-actin (Yang et al., 2020) that facilitate the protrusion of the cell membrane and the formation of invasive adhesions in solid tumours (Greaves and Calle, 2022). We then studied the possible co-expression of *VIM* with components and regulators of F-actin and other intermediate filament networks previously linked to the EMT phenotype.

Using the same *in silico* analysis approach, we found that the gene coding for (*NES*) was significantly co-expressed with *VIM* in all the solid tumours tested, whereas this correlation was not observed in AML or the other mesenchymal tumours analysed (Fig. 4A). The dynamics of F-actin in lamellipodia as well as in invadosomes (invadopodia and podosomes) is the result of the pattern of polymerisation of branched actin filaments. This process can be regulated by the available proportion of protein isoforms that comprise the Arp2/3 complex, which nucleates the polymerisation of branched F-actin (Abella et al., 2016). We then interrogated the cBioportal databases for possible differences in the co-expression of *VIM* and the Arp2/3 subunits and isoforms that may reflect specific changes in EMT-related migration between solid tumours and AML (Fig. 4 B-K). In all the epithelial tumours analysed, expression levels of *ACTR2* showed no significant correlation with the expression of *VIM* (Fig. 4 B). In two of the AML datasets, a weak positive correlation was observed whereas there was a negative correlation in mesenchymal

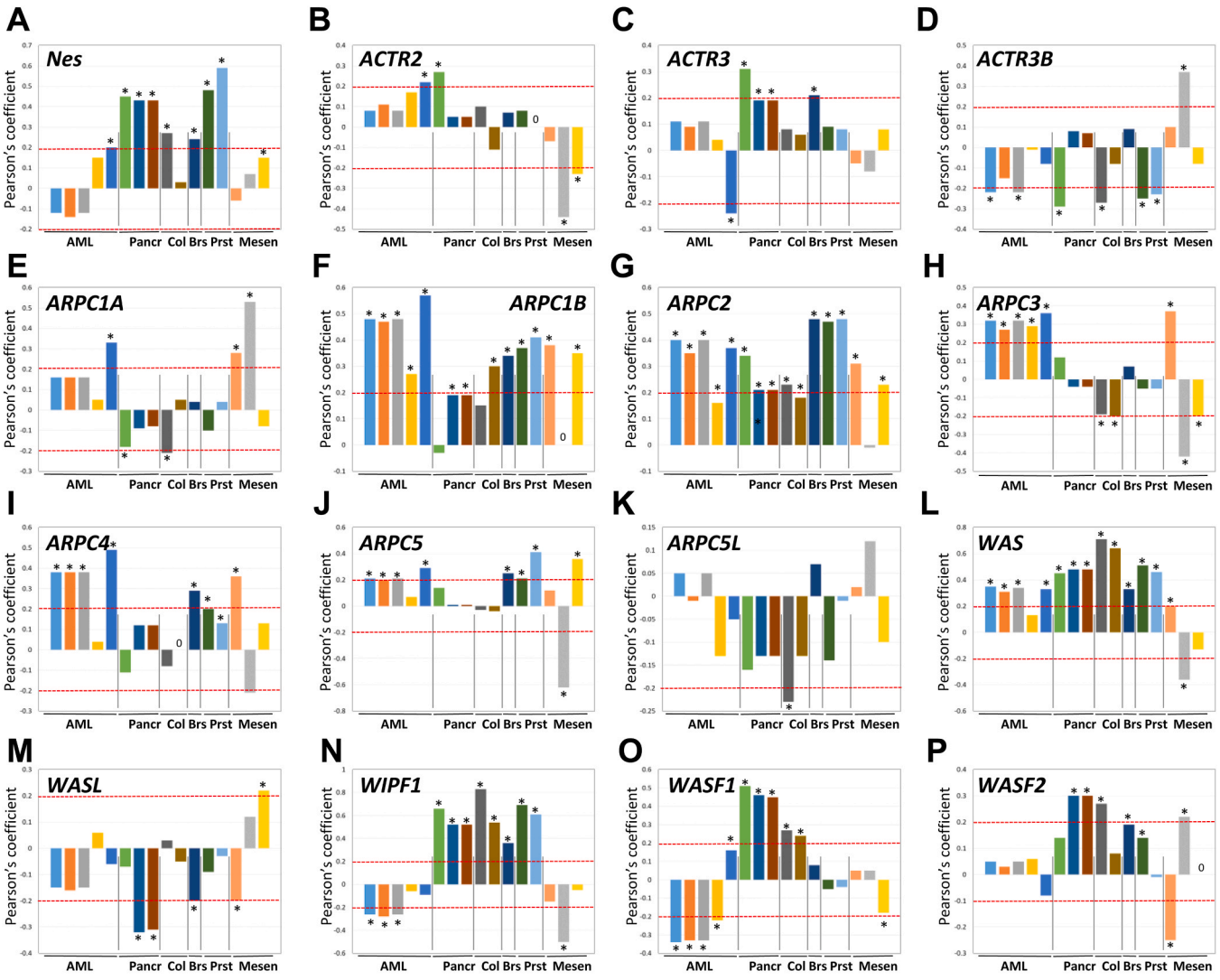

Fig. 4. Correlation between the mRNA expression of the *VIM* and genes coding for actin binding proteins. Graphs showing the Pearson's coefficient correlation values between the co-expression of *VIM* with (A) *Nes*, (B) *ACTR2*, (C) *ACTR3*, (D) *ACTR3B*, (E) *ARPC1A*, (F) *ARPC1B*, (G) *ARPC2*, (H) *ARPC3,* (I) *ARPC4*, (J) *ARPC5,* (K) *ARPC5L*, (L) *WAS*, (M) *WASL*, (N) *WIPF1*, (O) *WASF1* and (P) *WASF2* obtained with the bioinformatics tools in cBioportal using datasets specified in the graphs legend obtained from human cancer tumours of Acute Myeloid Leukaemia (AML), pancreatic carcinomas (Pancr), colorectal cancers (Col), breast (Brs), prostate (Prst) carcinomas and mesenchymal cancers (Mesen). * $p < 0.05$ correlation statistical significance. The red dash lines show the coefficient values of −0.2 and 0.2. The correlation values between −0.2 and 0.2 were considered too weak to reflect significant co-expressions; (Q) Western blot analysis showing the levels of expression of Arp2/3 proteins, WASP, WIP and ILK in eGFP-MOLM14 and eGFP-MV4–11 cultured alone or in the presence of mCherry-HS5 cells (+HS5). Asterisks point at the known calpain-cleavage fragment of WASP. Protein levels of β-actin were used as loading control.

tumours (Fig. 4 B). A very weak but consistent correlation with *ACTR3* expression was observed in pancreatic and breast cancer tumours whereas no consistent correlation was detected in the rest of the cancers analysed (Fig. 4C). AML tumours, colorectal and prostate carcinoma and one of the data sets of pancreatic cancer showed a weak inverse correlation in expression levels of *ACTR3B* and no clear pattern of co-expression could be determined in the other cancer types analysed (Fig. 4 D). A very weak pattern of co- expression of *ARPC1A* was observed in AML tumours that was stronger in mesenchymal tumours whereas prostate, breast and colorectal cancers did not show a clear correlation with expression of *VIM* (Fig. 4 E). However, expression of the *ARPC1B* isoform showed a clear positive correlation with the levels of expression of *VIM* across all the cancers tested (Fig. 4F) similarly to *ARPC2* (Fig. 4G). AML cancers also showed a clear correlation with the expression of *ARPC3* that was null or reverse in the other tumours analysed with exception of the dataset of paediatric acute lymphocytic leukaemia (Fig. 4 H). The same stronger positive correlation in AML tumours was observed with the expression of *ARPC4* and *ARPC5* in comparison to the other tumour analysed, except for the breast and prostate cancer tumours, which also showed, albeit weaker correlation with *ARPC4* and *ARPC5* (Fig. 4 I, J). The expression of *ARPC5L* showed a very weak but very consistent downregulation in all the epithelial tumours, except the breast cancer analysed and no correlation was observed in AML or mesenchymal tumours (Fig. 4K).

We tested whether some of the significant patterns of the co-expression of *VIM* with the Arp2/3 proteins identified *in silico* were reproduced in the revealed EMT-like phenotype induced in AML cells by BM-mesenchymal/fibroblastic cells. Mimicking the results *in silico*, the steep increase in VIM levels in AML cells induced by the co-culture setting was not mirrored by the variations of expression of ARPC1A and ARPC5L (Fig. 4 E, K, Q). The high degree of co-expression of *VIM* with *ARPC1B, ARPC3* and to some extent with *ARPC4* were also observed in AML cells co-cultured with BM mesenchymal/fibroblastic cells (Fig. 4F, H, I, Q). The tendency for the co-expression of *VIM* with *ARPC2* in AML cells in the *in silico* study was only reproduced *in vitro* with the cell line eGFP-MV4–11 (Fig. 4G, Q).

The WASP/WAVE family of proteins are key nucleation promoting factors that activate the Arp2/3 complex, playing a critical role in cell migration and signalling associated with various cell functions involved in cancer development and metastasis (Alekhina et al., 2017; Kurisu and Takenawa, 2010). Given that overall, our data indicate that AML and epithelial tumours seem to have different patterns of co-expression of *VIM* with the Arp2/3 subunits *ARPC3* and *ARPC4*, we explored whether there were also differences in relation to the expression of Arp2/3 activators (Izdebska et al., 2020). Interestingly, we found a clear pattern of co-expression of *WAS* with all the cancers studied, except for the melanoma and diffuse acute B-cell lymphoma tumours (Fig. 4L). The protein WASP (the product from the *WAS* gene) was initially thought to be expressed exclusively in haematopoietic cells whereas the protein N-WASP was the member of the same family that was ubiquitously expressed in all tissues (Calle et al., 2008). However, WASP has been reported to be upregulated in epithelial tumour cells (Schrank et al., 2018; Zhang et al., 2019). Our data corroborate previous studies associating the expression of WASP with epithelial cells displaying a mesenchymal (EMT-related) phenotype (Zhang et al., 2019). On the contrary, no significant correlation or an inverse correlation of *VIM* levels and *WASL* (the gene coding for N-WASP) was found in all the tumours analysed except for the melanoma and diffuse acute B-cell lymphoma tumour analysed (Fig. 4M). WASP and WIP (the protein coded by *WIPF1*) have been shown to work as a functional unit that regulates the organisation and dynamics of F-actin (Chou et al., 2006; de la Fuente et al., 2007). We found moderate and strong correlations between *VIM* levels and the expression of *WIPF1* in all the epithelial tumours tested, whereas this correlation was none or inversed in AML and the other mesenchymal tumours analysed (Fig. 4N). We also studied the variations in the levels of these critical Arp2/3 complex regulators in the AML cells undergoing an EMT-like process in the presence of BM mesenchymal/fibroblastic cells *vs* AML cultured alone. We found that WASP levels were sustained but not increased in the presence of BM stromal cells (Fig. 4 Q). However, the significant inverse co-expression of *VIM* and *WIP* in AML tumours detected *in silico* (Fig. 4N), was reproduced to a large extent in the AML cells co-cultured in the presence of BM stromal cells (Fig. 4 Q).

We also found a distinctive pattern of co-expression in AML cells of *VIM* and the isoforms of the Arp2/3 activators WAVE1 (protein coded by *WASF1*) and WAVE2 (protein coded by *WASF2*). A positive correlation was observed in epithelial tumours, stronger for *WASPF1*, that in AML tumours was inverse for *WASF1* (Fig. 4O) and null for *WASF2* (Fig. 4P). Mesenchymal tumours presented no correlation for *WASF1* (Fig. 4O) and not a clear pattern of correlation for *WASF2* (Fig. 4P).

Overall, our data show in AML tumours some specific patterns of co-expression with *VIM* with the subunits and isoforms of the Arp2/3 complex as well as with the levels of the Arp2/3 activators that are distinct from the ones observed in epithelial tumours. This pattern of co-expression identified *in silico* is largely induced in AML cells by BM mesenchymal/fibroblastic stromal cells.

3.4. Specific patterns of co-expression of VIM and components of invasive adhesions in AML in comparison to epithelial tumours

The size and dynamics of invadosomes are regulated by the associated cell adhesion molecules and interacting proteins (Linder et al., 2023). The same adhesion molecules can be clustered in invasive focal contacts also involved in the migration of cells undergoing EMT (Greaves and Calle, 2022). We reasoned that since invadosomes and invasive focal contacts can assemble during EMT the components of these adhesions associated with EMT may be upregulated or downregulated in parallel to VIM in order to modulate the function of EMT-related adhesion sites.

Integrin Linked Kinase (ILK) is a common component of integrin-mediated molecular platforms involved in the assembly of podosomes (Griera et al., 2014), invadopodia (McDonald and Dedhar, 2022) and invasive focal contacts (Li et al., 2007; McDonald and Dedhar, 2022), which is upregulated during EMT (McDonald and Dedhar, 2022). Our data show that expression of *ILK* correlates with *VIM* in all the tumours analysed (Fig. 5A). Our *in vitro* data also showed that the presence of BM mesenchymal/fibroblastic stromal cells also induced high levels of co-expression of ILK and VIM in AML cells (Fig. 4 Q). Interestingly, the genes coding for PINCH1 (*LIMS1*) and PARVIN (*PARVA*), two critical proteins that regulate ILK activity, presented a different pattern of co-expression *in silico*. *LIMS1* and *PARVA* were co-expressed with *VIM* in all epithelial tumours (except for *LIMS1* in prostate cancer) whereas their expression was inversely correlated in AML tumours and showed no clear correlation in the mesenchymal tumours analysed (Fig. 5 B, C).

Cortactin (coded by *CTTN*) is a regulator of F-actin dynamics that interacts with WIP in invadopodia and podosomes (Linder et al., 2023) and has been shown to participate in EMT (Ji et al., 2020). We found that *CTTN* was only co-expressed with *VIM* in mesenchymal tumours (Fig. 5 D) and presented a negative correlation in the AML tumours.

α-actinin (coded by *ACTN*) is an F-actin-bundling protein present in invadosomes (Linder et al., 2023) that is involved in EMT (Izdebska et al., 2020). We analysed the co-expression with *VIM* of its four known isoforms. We found a clear correlation of expression of *VIM* with *ACTN1* in all the epithelial and mesenchymal tumours analysed except to paediatric Acute Lymphocytic Leukaemia. In contrast, no correlation was observed in the AML tumours (Fig. 5 E). No significant patterns of correlation were observed with the *ACTN2* gene in any of the tumours studied (Fig. 5F). Similarly, no significant correlation with *ACTN3* was observed in AML tumours (Fig. 5G) while a positive weak correlation was detected in pancreatic, prostate and colorectal cancer. In contrast, a more consistent correlation with the expression of *ACTN4* was observed in AML cells in comparison to the rest of the tumour types analysed

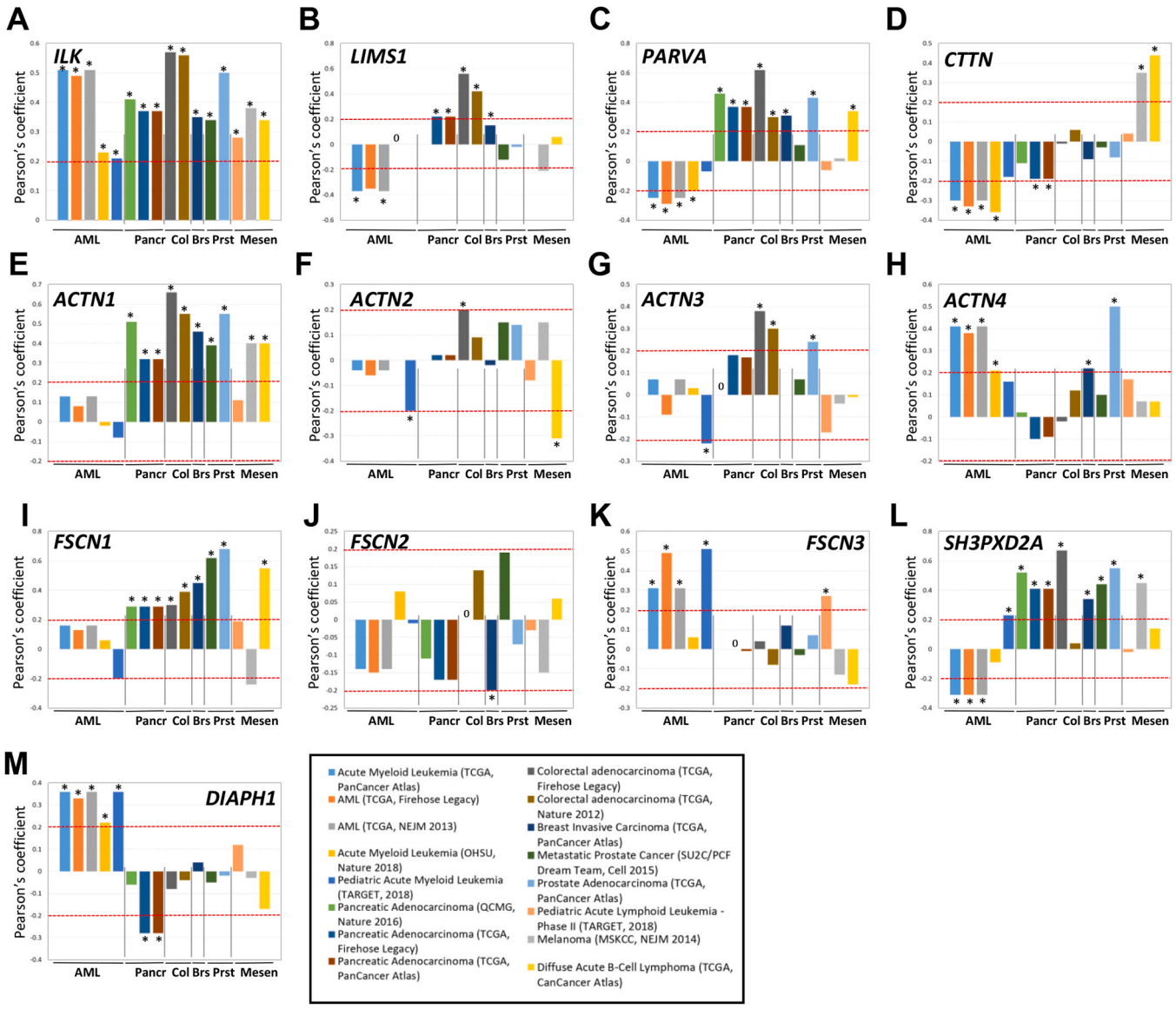

Fig. 5. Correlation between the mRNA expression of the *VIM* and genes coding for proteins involved in invadosome formation. Graphs showing the Pearson's coefficient correlation values between the co-expression of *VIM* with (A) *ILK*, (B) *LIMS1*, (C) *PARVA*, (D) *CTTN*, (E) *ACTN1*, (F) *ACTN2*, (G) *ACTN3*, (H) *ACTN4,* (I) *FSCN1*, (J) *FSCN2,* (K) *FSCN3*, (L) *SH3PXD2A* and (M) *DIAPH1* obtained with the bioinformatics tools in cBioportal using datasets specified in the graphs legend obtained from human cancer tumours of Acute Myeloid Leukaemia (AML), pancreatic carcinomas (Pancr), colorectal cancers (Col), breast (Brs), prostate (Prst) carcinomas and mesenchymal cancers (Mesen). * $p < 0.05$ correlation statistical significance. The red dash lines show the coefficient values of −0.2 and 0.2. The correlation values between −0.2 and 0.2 were considered too weak to reflect significant co-expressions. There were analysed genes that were not included in some of the databases and appear blank in the graphs.

Supplementary video 1. Time-lapse video of eGFP-MOLM14 cells seeded alone. Micrographs were acquired every minute for 15 min. The film shows a composite of phase contrast and eGFP fluorescence channel (green). Bar 50 μm.

Supplementary video 2. Time-lapse video of eGFP-MOLM14 cells seeded alone. Micrographs were acquired every minute for 15 min. The film shows the eGFP fluorescence channel (green). Bar 50 μm.

Supplementary video 3. Time-lapse video of eGFP-MOLM14 cells seeded in the presence of mCherry-HS5 cells. Micrographs were acquired every minute for 15 min. The film shows a composite of phase contrast and eGFP fluorescence channel (green) and mCherry (red). Bar 50 μm.

Suppleme ntary video 4. Time-lapse video of eGFP-MOLM14 cells seeded in the presence of mCherry-HS5 cells. Micrographs were acquired every minute for 15 min. The film shows a composite of phase contrast and eGFP fluorescence channel (green) and mCherry (red). Bar 50 μm.

(Fig. 5 H).

Expression of *FSCN1* and *FSCN1* (the genes coding for the isoforms 1 and 2 of F-actin-bundling protein fascin (Chung et al., 2022; Izdebska et al., 2020)) showed very weak or inverse co-expression with *VIM* in the AML tumours (Fig. 5 I, J). All the epithelial tumours presented a clear co-expression pattern of FSCN1 with VIM (Fig. 5 I). A distinctive significant correlation was observed with *FSCN3* in AML tumours while there was no significant correlation with the rest of tumour types analysed (Fig. 5K).

SH3PXD2A is the gene coding for TKS5, a critical regulator of podosome and invadopodia formation (Linder et al., 2023). *SH3PXD2A* showed a specific pattern of inverse co-expression with *VIM* in AML cells in contrast with the positive moderate correlation detected in the great majority of the rest of the tumours analysed (Fig. 5L).

Finally, we found that *DIAPH1*, the gene coding for the actin polymerising factor DIA/DF1 showed a moderate correlation with the

expression levels of *VIM* in the AML tumours whereas it showed a null or inverse correlation in the rest of the tumours under study (Fig. 5M).

Taken together our data also show that AML present specific patterns of co-expression of *VIM* with the transcripts coding for proteins that regulate the structure and dynamics of invadosomes (*LIMS1*, *PARVA*, *ACTN3* and *4*, *FSCN1* and *3*, *SH3PXD2A* and *DIAPH1*) that are distinct from the patterns observed in epithelial tumours.

4. Discussion

Similarly to MM (Ghobrial, 2012), leukaemia can be envisaged as a model for metastatic cancer (Whiteley et al., 2021) in which the migratory capacity of leukaemia cells plays a critical role in disease progression and drug resistance by facilitating cancer cell dissemination to new sites and the interaction with cytoprotective tissue niches (Whiteley et al., 2021). In AML, compelling evidence indicates that upregulation of EMT markers enhances the migratory capacity of AML blasts (Kahlert et al., 2017) and correlates with poor prognosis (Stavropoulou et al., 2016; Wu et al., 2018). However, the triggering factors and signalling pathways involved in development of EMT in AML cells remain largely unknown (Greaves and Calle, 2022). The BM microenvironment has been shown to induce EMT in MM by providing a hypoxic environment and through the secretion of extracellular matrix proteins by BM mesenchymal/fibroblastic stromal cells that promote migration of MM cells (Azab et al., 2012; Ibraheem et al., 2019). Hypoxia has also been shown to induce EMT in AML (Jiang et al., 2021; Percio et al., 2014). In the current work, we have explored the possible role of BM mesenchymal/fibroblastic stromal cells in regulating AML migration through the activation of an EMT program.

We found that BM mesenchymal/fibroblastic stromal cells promote migration of AML cells in a process linked to the increased release of MMP-2 and MMP-9 to the extracellular milieu. Our results suggest that AML cells are responsible for the increased secretion of MMP-9 in our experimental setting. It is likely that in co-culture, mCherry-HS5 cells secrete the detected pro-MMP-2 as high levels of pro-MMP-2 were detected in the culture media of these cells cultured alone. However, we cannot discard a possible secretion of MMP-2 by AML cells (Chaudhary et al., 2016; Sawicki et al., 1998). A similar pattern of secretion of active MMP-2 in co-culture of BM stromal and AML cells *vs* BM stromal cells cultured alone has been previously reported in BM cultures from AML patients (Janowska-Wieczorek et al., 1999). The secretion of MMP-9 and MMP-2 has previously been linked to the invasive migration of AML cells as well as to tumour progression (Chaudhary et al., 2016; Pirillo et al., 2022; Sawicki et al., 1998; Tavor et al., 2005; Zhang et al., 2004) and poor responses to therapy (Song et al., 2009). MMP-2 and MMP-9 may promote the remodelling of the extracellular matrix and/or the activation of matrix-associated soluble factors such as TGFβ1 (Horiguchi et al., 2012) that could further promote AML migration and mobilisation. It has also been shown that MMPs can increase vascular leakiness contributing to AML mobilisation, loss of normal haematopoietic stem cells from the BM and disease progression (Pirillo et al., 2022). Overall, our results suggest that the crosstalk between AML cells and protective BM stromal cells prompts the migration of AML cells and the secretion of MMP-2 and MMP-9. This increase in protease secretion may contribute to the MMP-dependent mode of migration of AML cells and the remodelling of the BM microenvironment that facilitates disease progression.

Secretion of MMPs is linked to the mesenchymal mode of migration and AML cells have been shown to express high levels of EMT markers in patients with poor prognosis (Stavropoulou et al., 2016). Additionally, detection of high levels of expression of *VIM* (Wu et al., 2018) and downregulation of E-cadherin (Zhang et al., 2017) in AML blasts from patients correlates with poor clinical outcomes. Hence, we decided to investigate whether the increased migratory phenotype of AML cells induced in co-culture with BM stromal cells correlated with the changes in expression of classical EMT markers. We detected a highly significant increase in VIM levels in AML cells in co-culture mirrored by an increase in expression of N-cadherin occurring in parallel to the repression of the expression of E-cadherin. In contrast, the increase in the EMT-related transcription factors SNAI1 and SNAI2 was very modest in comparison. Since AML cells are mesenchymal, it is not surprising that the pattern of activation of some EMT markers when cells may undergo EMT may differ from those previously characterised in epithelial tumours (Yang et al., 2020). The most recent consensus in the EMT field is that non-epithelial tumours may undergo particular patterns of expression of EMT markers that equally result in a migratory EMT-like phenotype (Yang et al., 2020). In AML cells, the fact that the levels of some core EMT markers such as SNAI1 and SNAI2 may not vary to the same extent as VIM, does not imply that they may not have critical roles in the AML EMT phenotype (Carmichael et al., 2020; Zhang et al., 2020). It is possible that particular configurations of co-expression of EMT markers may result in different molecular landscapes that could explain the pattern of cancer cell plasticity associated to specific tumours. A recent report in breast cancer indicates that even within the same tumour type, cancer cells can undergo different "EMT trajectories" (different patterns of co-expression of EMT markers) that may be determined by the cellular composition of the surrounding TME (Malagoli Tagliazucchi et al., 2023). Hence, the activation of regulatory networks resulting from these co-expression patterns of EMT-related genes may regulate in cancer cells their migratory phenotype and adaptation to the interaction with the surrounding tissues. These processes may contribute to cell plasticity related to drug resistance and ultimately limit the response of AML cells to therapy (Pastushenko and Blanpain, 2019). Importantly, our data indicate that the interaction of AML cells with BM mesenchymal/fibroblastic cells promotes the development of an EMT-like phenotype in AML cells. Cancer cells undergoing EMT processes are more resistant to radiotherapy and drug treatments (Yang et al., 2020). It is possible that the identified EMT-process induced in AML cells by BM mesenchymal/fibroblastic cells may contribute to their cytoprotective role against drug treatments (Arroyo-Berdugo et al., 2023). Understanding the signalling pathways involved in the EMT-like processes in AML induced by the BM microenvironment may lead to the identification of targets for new therapeutic interventions to overcome drug resistance in AML.

In order to validate the observed pattern of relative expression of VIM and SNAI1 and SNAI2 in AML and to identify other possible distinct co-expression patterns of VIM with core EMT markers, we performed an *in silico* analysis using datasets of mRNA levels obtained from Human AML tumours *vs* tumours of epithelial and mesenchymal origin. AML and epithelial tumours showed the expected pattern of positive and negative co-expression of *VIM* with *CDH1* and *CDH2*, respectively. This pattern of expression of *CDH1* and *CDH2* related to EMT may regulate progression of AML tumours. For example, expression of limited levels of *CDH1* has been associated with poor prognosis in AML (Zhang et al., 2017) and clustering of CDH2 has been shown to regulate the trafficking of AML cells to the BM (Marjon et al., 2016) while high expression correlates with poor prognosis (Qu et al., 2023).

As previously reported, we corroborated that the expression of the core EMT markers *SNAI1, SNAI2, ZEB1, ZEB2, TWIST1 and TWIST2* clearly correlated with increased levels of *VIM* in all the epithelial tumours tested (Yang et al., 2020). In contrast AML tumours showed a distinct null and even reverse correlation, between expression of these markers and *VIM*. These results validate our *in vitro* data showing the particular modulation of VIM with respect to the levels of SNAI1 and SNAI2 in AML cells undergoing EMT induced by BM mesenchymal/fibroblastic cells. It is likely that the core EMT markers are differentially controlled in non-migratory (when *VIM* levels are very low) vs migratory AML cells and may involve signalling networks that may differ from those in epithelial tumours. Determining these possible differences in the mechanism of regulation of the activity of EMT markers between cancers should lead to a better understanding of the cancer-type associated EMT states and to the development of tailored anti-metastatic and

tumour progression therapies. Additionally, regulation of *VIM* levels in AML may be regulated by alternative pathways. For example, the transcription factor HOXA9 can regulate the expression of VIM and N-cadherin (Xu et al., 2021). Expression of the oncogenic fusion protein MLL-AF9 in haematopoietic stem cells leads to the development of aggressive AML tumours showing high expression levels of *HOXA9* and *VIM* as well as other EMT markers that also correlate with poor prognosis in patients (Stavropoulou et al., 2016). Finally, our data indicate that BM mesenchymal/fibroblastic cells induce the expression of VIM correlating with the development of an EMT-like mode of migration (integrin, MMP and Src-activity dependent) in AML cells. However, it is possible that similarly to healthy myeloid cells (Shaebani et al., 2022) and other cancer cells (Lavenus et al., 2020), when exposed to confined environments AML cells may have the capacity to switch to an amoeboid mode of migration (integrin, MMP and Src-activity independent), which can also be regulated by VIM (Lavenus et al., 2020; Shaebani et al., 2022).

EMT-related migration involves the polymerisation of upregulated VIM into filaments in coordination with the rearrangement of the other cytoskeletal networks (Greaves and Calle, 2022). We showed that the presence of BM fibroblastic stromal cells induce both the upregulation of VIM and the formation of VIM filaments in migrating AML cells.

Rearrangement of F-actin also occurs in coordination with the upregulation of VIM during EMT (Izdebska et al., 2020; Yang et al., 2020). The protrusive activity of the leading edge of migrating cells is powered by the polymerisation of branched F-actin. This process is regulated by the activity of the actin polymerising factor Arp2/3 complex (Abella et al., 2016), which is activated by the families of nucleation promoting factors (Biber et al., 2020). We explored whether the co-expression of *VIM* and the proteins involved in F-actin and adhesion remodelling also presented particular patterns in AML cells vs epithelial tumours related to a differential regulation of the F-actin polymerising machinery to facilitate the different patterns of interaction of AML cells with the surrounding tissues (Greaves and Calle, 2022). The proportion of the subunit isoforms present in the Arp2/3 complex affects the structure and dynamics of F-actin (Abella et al., 2016). We found a common pattern of co-expression of *VIM* with the *ARPC1B* isoform and the *ARPC2* subunit in all the cancers studied. These two subunits of the Arp2/3 complex have been shown to play a role in cancer. Upregulation of ARPC1B has been shown to promote oncogenesis and EMT cell migration in prostate (Gamallat et al., 2022), glioma (Gao et al., 2022), glioblastoma (Liu et al., 2022) as well as resistance to radiotherapy (Gao et al., 2022; Kumagai et al., 2006). ARPC1B enhances the activity of the Arp2/3 complex in comparison with its isoform ARPC1A (von Loeffelholz et al., 2020). Expression of high levels of ARPC2 has been shown to promote breast cancer cell EMT migration and metastasis (Cheng et al., 2019). In addition to its role in promoting actin polymerisation contributing to EMT, the ectopic expression of ARPC2 has been shown to induce the expression of the mesenchymal markers N-cadherin and VIM (Cheng et al., 2019) further associating its expression to regulation of EMT. Moreover, inhibition of ARPC2 activity restricts the migration of lung, pancreas and colon cancers (Choi et al., 2019). Taken together, these results suggest that upregulation of *VIM* occurs in parallel with the expression of the isoforms of the Arp2/3 complex subunits that would facilitate enhanced actin polymerisation.

In addition, we have also identified distinct patterns of expression of Arp2/3 subunits associated to AML cancers with increased co-expression of *ARPC1A*, *ARPC3* and *ARPC4* with *VIM vs* epithelial tumours. To our knowledge, none of these Arp2/3 subunits have been shown to play a role in AML. However, these three subunits have been related to cancer cell migration and invasion in other tumour types (Laurila et al., 2009; Rauhala et al., 2013). We found that BM mesenchymal/fibroblastic stromal cells induce the co-expression of VIM with ARPC1A, ARPC3 and ARPC4 in AML cells correlating with the development of a migratory EMT-like phenotype. Future studies should address the possible specific role of these isoforms in AML migration and progression and their possible significance for the design of therapeutic interventions to block EMT-mediated drug resistance.

The Arp2/3 complex becomes active by binding to nucleation promoting factors such as the WASP/WAVE family of proteins, which have also been involved in carcinogenesis (Izdebska et al., 2020). Our data also show a clear co-upregulation of *WAS* (coding for WASP) with *VIM* in the majority of the tumours studied. Interestingly, *ARPC1B*, whose transcript we found co-expressed with *VIM* similarly to the pattern of *WAS*, has been shown to interact with WASP and promote its Arp2/3 complex activating function during podosome formation (Leung et al., 2021). The enhanced activity of the Arp 2/3 complex mediated by WASP may be a possible mechanism of activation of F-actin dynamics during EMT that parallels upregulation of *VIM* that may be common to epithelial tumours and AML. However, the regulation of WASP in AML cells may differ from epithelial tumours since the gene coding for the protein WIP (*WIPF1*), which plays a critical role in the maintenance of WASP stability and subcellular localisation (Chou et al., 2006; de la Fuente et al., 2007), showed in our *in silico* studies a pattern of inverse co-expression with *VIM* in AML cells whereas it mirrored the expression of *VIM* in epithelial tumours. WIP has previously been shown to drive oncogenesis in several solid tumours (Escoll et al., 2017; Gargini et al., 2016; Menotti et al., 2019; Salvi and Thanabalu, 2017) while in some haematological malignancies (Pereira et al., 2017; Wang et al., 2021) and in lymphoma (Menotti et al., 2019) WIP and WASP work as tumour suppressors. Our data suggest that the role and regulation of WASP and WIP in AML may differ from other haematological malignancies. We found that similarly to the observations in other haematological malignancies, WIP may be expressed at lower levels in aggressive forms of AML with an invasive EMT profile rich in VIM. However, our results revealed a co-expression between the gene coding for WASP (*WAS*) and *VIM* in AML. Our data also indicate that BM mesenchymal/fibroblastic cells contribute to the regulation of the reverse co-expression of WIP with VIM while they hardly affected the expression of WASP. This suggests that perhaps other BM microenvironment components may be the major contributors to the modulation of WASP levels during the development of the EMT-like phenotype in AML. The exact role and mechanisms of regulation of WASP and WIP in AML should be further studied to clarify their exact role in EMT and tumour progression.

The variations in the patterns of co-expression of epithelial and mesenchymal markers (Pastushenko and Blanpain, 2019; Pastushenko et al., 2018) may also explain the specific configuration of cell adhesion molecules and associated proteins assembled during EMT migration in different tumour types (Greaves and Calle, 2022). Integrins and associated proteins are critical for the formation of the variety of cell adhesions including invadopodia, podosomes and invasive focal contacts formed in cancer cells undergoing EMT processes. All the tumours analysed in our *in silico* study including AML showed an upregulation of *ILK*, which correlates with the involvement of integrin-mediated migration in the EMT processes developed. We also found that BM mesenchymal stromal cells promote the co-expression of VIM and ILK in AML cells. However, given the differences between AML and the epithelial tumours in the co-expression of the genes *LIMS1 and PARVA*, which code for the ILK interacting proteins PINCH1 and parvin, it is likely that the integrin-mediated adhesions are distinctively organised and/or controlled in AML vs epithelial tumours. The difference in co-expression of *VIM* with *ACTN1, 3* and *4*, *FSCN1* and *3*, *SH3PXD2A* and *DIAPH1* in AML *vs* epithelial tumours also suggest the specific regulation of the organisation and dynamics of F-actin. The resulting cytoskeletal and adhesion configuration will ultimately control the specific migration patterns that may be associated with tissue invasion and lodging to form secondary tumours of AML.

5. Conclusions

In summary, our findings further support the existence of cancer-type specific modes of EMT (Yang et al., 2020) that result from

distinct patterns of coordinated expression of cytoskeletal and adhesion proteins. These patterns may be determined by the specific regulation of core EMT markers. Specifically, we show that in response to the stimulation by BM mesenchymal/fibroblastic cells, AML cancer cells can undergo an EMT-like phenotype that results from a strong upregulation of *VIM* that does not correlate with the upregulation of some core EMT markers observed in epithelial tumours. This process also involves some distinct patterns of co-expression of actin binding and adhesion proteins that regulate F-actin dynamics. These results warrant future investigations to identify and further characterise the signalling networks activated to induce these processes in order to devise new tailored therapies for AML as well as different types of cancer.

Funding

This research received funding from Cancer Research UK (reference C34579/A20784) and from the funds for research-led teaching activities from the University of Roehampton.

CRediT authorship contribution statement

Natalia Nojszewska: Investigation, formal analysis. Orest Idilli: Investigation, formal analysis. Debalina Sarkar: Investigation, formal analysis. Zaynab Ahouiyek: Investigation, formal analysis. Yoana Arroyo-Berdugo: Investigation, writing - review & editing Maryam S Amin-Anjum: Investigation. Sean Bowers: Investigation. David Greaves: Investigation. Ladan Saeed: Investigation. Mohsin Khan: Investigation. Sara Salti: Investigation. Sara Al-Shami: Investigation. Helin Topoglu: Investigation. John K Punzalan: Investigation. Cristian Sandoval: Investigation. Jorge G. Farias: Analysis, review & editing of the drafts. Yolanda Calle: Conceptualization, funding acquisition, investigation, formal analysis, writing - original draft and review & editing.

Declaration of Competing Interest

None.

Data Availability

Data will be made available on request.

Appendix A. Supporting information

Supplementary data associated with this article can be found in the online version at doi:10.1016/j.ejcb.2023.151334.

References

Abella, J.V., Galloni, C., Pernier, J., Barry, D.J., Kjaer, S., Carlier, M.F., Way, M., 2016. Isoform diversity in the Arp2/3 complex determines actin filament dynamics. Nat. Cell Biol. 18, 76–86.

Alekhina, O., Burstein, E., Billadeau, D.D., 2017. Cellular functions of WASP family proteins at a glance. J. Cell Sci. 130, 2235–2241.

Arroyo-Berdugo, Y., Sendino, M., Greaves, D., Nojszewska, N., Idilli, O., So, C.W., Di Silvio, L., Quartey-Papafio, R., Farzaneh, F., Rodriguez, J.A., Calle, Y., 2023. High throughput fluorescence-based in vitro experimental platform for the identification of effective therapies to overcome tumour microenvironment-mediated drug resistance in AML. Cancers (Basel) 15.

Attieh, Y., Vignjevic, D.M., 2016. The hallmarks of CAFs in cancer invasion. Eur. J. Cell Biol. 95, 493–502.

Azab, A.K., Hu, J., Quang, P., Azab, F., Pitsillides, C., Awwad, R., Thompson, B., Maiso, P., Sun, J.D., Hart, C.P., Roccaro, A.M., Sacco, A., Ngo, H.T., Lin, C.P., Kung, A.L., Carrasco, R.D., Vanderkerken, K., Ghobrial, I.M., 2012. Hypoxia promotes dissemination of multiple myeloma through acquisition of epithelial to mesenchymal transition-like features. Blood 119, 5782–5794.

Bailey, P., Chang, D.K., Nones, K., Johns, A.L., Patch, A.M., Gingras, M.C., Miller, D.K., Christ, A.N., Bruxner, T.J., Quinn, M.C., Nourse, C., Murtaugh, L.C., Harliwong, I., Idrisoglu, S., Manning, S., Nourbakhsh, E., Wani, S., Fink, L., Holmes, O., Chin, V., Anderson, M.J., Kazakoff, S., Leonard, C., Newell, F., Waddell, N., Wood, S., Xu, Q., Wilson, P.J., Cloonan, N., Kassahn, K.S., Taylor, D., Quek, K., Robertson, A., Pantano, L., Mincarelli, L., Sanchez, L.N., Evers, L., Wu, J., Pinese, M., Cowley, M.J., Jones, M.D., Colvin, E.K., Nagrial, A.M., Humphrey, E.S., Chantrill, L.A., Mawson, A., Humphris, J., Chou, A., Pajic, M., Scarlett, C.J., Pinho, A.V., Giry-Laterriere, M., Rooman, I., Samra, J.S., Kench, J.G., Lovell, J.A., Merrett, N.D., Toon, C.W., Epari, K., Nguyen, N.Q., Barbour, A., Zeps, N., Moran-Jones, K., Jamieson, N.B., Graham, J.S., Duthie, F., Oien, K., Hair, J., Grutzmann, R., Maitra, A., Iacobuzio-Donahue, C.A., Wolfgang, C.L., Morgan, R.A., Lawlor, R.T., Corbo, V., Bassi, C., Rusev, B., Capelli, P., Salvia, R., Tortora, G., Mukhopadhyay, D., Petersen, G.M., Australian Pancreatic Cancer Genome, I., Munzy, D.M., Fisher, W.E., Karim, S.A., Eshleman, J.R., Hruban, R.H., Pilarsky, C., Morton, J.P., Sansom, O.J., Scarpa, A., Musgrove, E.A., Bailey, U.M., Hofmann, O., Sutherland, R.L., Wheeler, D. A., Gill, A.J., Gibbs, R.A., Pearson, J.V., et al., 2016. Genomic analyses identify molecular subtypes of pancreatic cancer. Nature 531, 47–52.

Biber, G., Ben-Shmuel, A., Sabag, B., Barda-Saad, M., 2020. Actin regulators in cancer progression and metastases: from structure and function to cytoskeletal dynamics. Int Rev. Cell Mol. Biol. 356, 131–196.

Biber, G., Ben-Shmuel, A., Noy, E., Joseph, N., Puthenveetil, A., Reiss, N., Levy, O., Lazar, I., Feiglin, A., Ofran, Y., Kedmi, M., Avigdor, A., Fried, S., Barda-Saad, M., 2021. Targeting the actin nucleation promoting factor WASp provides a therapeutic approach for hematopoietic malignancies. Nat. Commun. 12, 5581.

Calle, Y., Anton, I.M., Thrasher, A.J., Jones, G.E., 2008. WASP and WIP regulate podosomes in migrating leukocytes. J. Microsc. 231, 494–505.

Cancer Genome Atlas, N., 2012. Comprehensive molecular characterization of human colon and rectal cancer. Nature 487, 330–337.

Cancer Genome Atlas Research, N, Ley, T.J., Miller, C., Ding, L., Raphael, B.J., Mungall, A.J., Robertson, A., Hoadley, K., Triche Jr., T.J., Laird, P.W., Baty, J.D., Fulton, L.L., Fulton, R., Heath, S.E., Kalicki-Veizer, J., Kandoth, C., Klco, J.M., Koboldt, D.C., Kanchi, K.L., Kulkarni, S., Lamprecht, T.L., Larson, D.E., Lin, L., Lu, C., McLellan, M.D., McMichael, J.F., Payton, J., Schmidt, H., Spencer, D.H., Tomasson, M.H., Wallis, J.W., Wartman, L.D., Watson, M.A., Welch, J., Wendl, M.C., Ally, A., Balasundaram, M., Birol, I., Butterfield, Y., Chiu, R., Chu, A., Chuah, E., Chun, H.J., Corbett, R., Dhalla, N., Guin, R., He, A., Hirst, C., Hirst, M., Holt, R.A., Jones, S., Karsan, A., Lee, D., Li, H.I., Marra, M.A., Mayo, M., Moore, R.A., Mungall, K., Parker, J., Pleasance, E., Plettner, P., Schein, J., Stoll, D., Swanson, L., Tam, A., Thiessen, N., Varhol, R., Wye, N., Zhao, Y., Gabriel, S., Getz, G., Sougnez, C., Zou, L., Leiserson, M.D., Vandin, F., Wu, H.T., Applebaum, F., Baylin, S. B., Akbani, R., Broom, B.M., Chen, K., Motter, T.C., Nguyen, K., Weinstein, J.N., Zhang, N., Ferguson, M.L., Adams, C., Black, A., Bowen, J., Gastier-Foster, J., Grossman, T., Lichtenberg, T., Wise, L., Davidsen, T., Demchok, J.A., Shaw, K.R., Sheth, M., Sofia, H.J., Yang, L., Downing, J.R., et al., 2013. Genomic and epigenomic landscapes of adult de novo acute myeloid leukemia. N. Engl. J. Med. 368, 2059–2074.

Carmichael, C.L., Wang, J., Nguyen, T., Kolawole, O., Benyoucef, A., De Maziere, C., Milne, A.R., Samuel, S., Gillinder, K., Hediyeh-Zadeh, S., Vo, A.N.Q., Huang, Y., Knezevic, K., McInnes, W.R.L., Shields, B.J., Mitchell, H., Ritchie, M.E., Lammens, T., Lintermans, B., Van Vlierberghe, P., Wong, N.C., Haigh, K., Thoms, J.A.I., Toulmin, E., Curtis, D.J., Oxley, E.P., Dickins, R.A., Beck, D., Perkins, A., McCormack, M.P., Davis, M.J., Berx, G., Zuber, J., Pimanda, J.E., Kile, B.T., Goossens, S., Haigh, J.J., 2020. The EMT modulator SNAI1 contributes to AML pathogenesis via its interaction with LSD1. Blood 136, 957–973.

Cerami, E., Gao, J., Dogrusoz, U., Gross, B.E., Sumer, S.O., Aksoy, B.A., Jacobsen, A., Byrne, C.J., Heuer, M.L., Larsson, E., Antipin, Y., Reva, B., Goldberg, A.P., Sander, C., Schultz, N., 2012. The cBio cancer genomics portal: an open platform for exploring multidimensional cancer genomics data. Cancer Discov. 2, 401–404.

Chaudhary, A.K., Chaudhary, S., Ghosh, K., Shanmukaiah, C., Nadkarni, A.H., 2016. Secretion and expression of matrix metalloproteinase-2 and 9 from bone marrow mononuclear cells in myelodysplastic syndrome and acute Myeloid Leukemia. Asian Pac. J. Cancer Prev. 17, 1519–1529.

Cheng, Z., Wei, W., Wu, Z., Wang, J., Ding, X., Sheng, Y., Han, Y., Wu, Q., 2019. ARPC2 promotes breast cancer proliferation and metastasis. Oncol. Rep. 41, 3189–3200.

Cheong, C.M., Mrozik, K.M., Hewett, D.R., Bell, E., Panagopoulos, V., Noll, J.E., Licht, J. D., Gronthos, S., Zannettino, A.C.W., Vandyke, K., 2020. Twist-1 is upregulated by NSD2 and contributes to tumour dissemination and an epithelial-mesenchymal transition-like gene expression signature in t(4;14)-positive multiple myeloma. Cancer Lett. 475, 99–108.

Choi, B.J., Park, S.A., Lee, S.Y., Cha, Y.N., Surh, Y.J., 2017. Hypoxia induces epithelial-mesenchymal transition in colorectal cancer cells through ubiquitin-specific protease 47-mediated stabilization of Snail: a potential role of Sox9. Sci. Rep. 7, 15918.

Choi, J., Lee, Y.J., Yoon, Y.J., Kim, C.H., Park, S.J., Kim, S.Y., Doo Kim, N., Cho Han, D., Kwon, B.M., 2019. Pimozide suppresses cancer cell migration and tumor metastasis through binding to ARPC2, a subunit of the Arp2/3 complex. Cancer Sci. 110, 3788–3801.

Chou, H.C., Anton, I.M., Holt, M.R., Curcio, C., Lanzardo, S., Worth, A., Burns, S., Thrasher, A.J., Jones, G.E., Calle, Y., 2006. WIP regulates the stability and localization of WASP to podosomes in migrating dendritic cells. Curr. Biol.: CB 16, 2337–2344.

Chung, J.M., Sato, O., Ikebe, R., Lee, S., Ikebe, M., Jung, H.S., 2022. Structural analysis of human fascin-1: essential protein for actin filaments bundling. Life (Basel) 12.

Dai, J., Qin, L., Chen, Y., Wang, H., Lin, G., Li, X., Liao, H., Fang, H., 2019. Matrix stiffness regulates epithelial-mesenchymal transition via cytoskeletal remodeling and MRTF-a translocation in osteosarcoma cells. J. Mech. Behav. Biomed. Mater. 90, 226–238.

Escoll, M., Gargini, R., Cuadrado, A., Anton, I.M., Wandosell, F., 2017. Mutant p53 oncogenic functions in cancer stem cells are regulated by WIP through YAP/TAZ. Oncogene 36, 3515–3527.

Fattet, L., Jung, H.Y., Matsumoto, M.W., Aubol, B.E., Kumar, A., Adams, J.A., Chen, A.C., Sah, R.L., Engler, A.J., Pasquale, E.B., Yang, J., 2020. Matrix rigidity controls

epithelial-mesenchymal plasticity and tumor metastasis via a mechanoresponsive EPHA2/LYN complex. Dev. Cell 54, 302–316 e307.
Fiori, M.E., Di Franco, S., Villanova, L., Bianca, P., Stassi, G., De Maria, R., 2019. Cancer-associated fibroblasts as abettors of tumor progression at the crossroads of EMT and therapy resistance. Mol. Cancer 18, 70.
de la Fuente, M.A., Sasahara, Y., Calamito, M., Anton, I.M., Elkhal, A., Gallego, M.D., Suresh, K., Siminovitch, K., Ochs, H.D., Anderson, K.C., Rosen, F.S., Geha, R.S., Ramesh, N., 2007. WIP is a chaperone for Wiskott-Aldrich syndrome protein (WASP). Proc. Natl. Acad. Sci. U. S. A. 104, 926–931.
Galeaz, C., Totis, C., Bisio, A., 2021. Radiation resistance: a matter of transcription factors. Front Oncol. 11, 662840.
Gamallat, Y., Zaaluk, H., Kish, E.K., Abdelsalam, R., Liosis, K., Ghosh, S., Bismar, T.A., 2022. ARPC1B is associated with lethal prostate cancer and its inhibition decreases cell invasion and migration in vitro. Int. J. Mol. Sci. 23.
Gao, J., Aksoy, B.A., Dogrusoz, U., Dresdner, G., Gross, B., Sumer, S.O., Sun, Y., Jacobsen, A., Sinha, R., Larsson, E., Cerami, E., Sander, C., Schultz, N., 2013. Integrative analysis of complex cancer genomics and clinical profiles using the cBioPortal. Sci. Signal 6, pl1.
Gao, Z., Xu, J., Fan, Y., Zhang, Z., Wang, H., Qian, M., Zhang, P., Deng, L., Shen, J., Xue, H., Zhao, R., Zhou, T., Guo, X., Li, G., 2022. ARPC1B promotes mesenchymal phenotype maintenance and radiotherapy resistance by blocking TRIM21-mediated degradation of IFI16 and HuR in glioma stem cells. J. Exp. Clin. Cancer Res 41, 323.
Gargini, R., Escoll, M., Garcia, E., Garcia-Escudero, R., Wandosell, F., Anton, I.M., 2016. WIP drives tumor progression through YAP/TAZ-dependent autonomous cell growth. Cell Rep. 17, 1962–1977.
Ghobrial, I.M., 2012. Myeloma as a model for the process of metastasis: implications for therapy. Blood 120, 20–30.
Greaves, D., Calle, Y., 2022. Epithelial Mesenchymal Transition (EMT) and associated invasive adhesions in solid and haematological tumours. Cells 11.
Griera, M., Martin-Villar, E., Banon-Rodriguez, I., Blundell, M.P., Jones, G.E., Anton, I. M., Thrasher, A.J., Rodriguez-Puyol, M., Calle, Y., 2014. Integrin linked kinase (ILK) regulates podosome maturation and stability in dendritic cells. Int. J. Biochem. Cell Biol. 50, 47–54.
Guo, W., Keckesova, Z., Donaher, J.L., Shibue, T., Tischler, V., Reinhardt, F., Itzkovitz, S., Noske, A., Zurrer-Hardi, U., Bell, G., Tam, W.L., Mani, S.A., van Oudenaarden, A., Weinberg, R.A., 2012. Slug and Sox9 cooperatively determine the mammary stem cell state. Cell 148, 1015–1028.
Horiguchi, M., Ota, M., Rifkin, D.B., 2012. Matrix control of transforming growth factor-beta function. J. Biochem. 152, 321–329.
Ibraheem, A., Attar-Schneider, O., Dabbah, M., Dolberg Jarchowsky, O., Tartakover Matalon, S., Lishner, M., Drucker, L., 2019. BM-MSCs-derived ECM modifies multiple myeloma phenotype and drug response in a source-dependent manner. Transl. Res. 207, 83–95.
Ishiwata, T., 2016. Cancer stem cells and epithelial-mesenchymal transition: novel therapeutic targets for cancer. Pathol. Int 66, 601–608.
Izdebska, M., Zielinska, W., Halas-Wisniewska, M., Grzanka, A., 2020. Involvement of actin and actin-binding proteins in carcinogenesis. Cells 9.
Janowska-Wieczorek, A., Marquez, L.A., Matsuzaki, A., Hashmi, H.R., Larratt, L.M., Boshkov, L.M., Turner, A.R., Zhang, M.C., Edwards, D.R., Kossakowska, A.E., 1999. Expression of matrix metalloproteinases (MMP-2 and -9) and tissue inhibitors of metalloproteinases (TIMP-1 and -2) in acute myelogenous leukaemia blasts: comparison with normal bone marrow cells. Br. J. Haematol. 105, 402–411.
Ji, R., Zhu, X.J., Wang, Z.R., Huang, L.Q., 2020. Cortactin in epithelial-mesenchymal transition. Front Cell Dev. Biol. 8, 585619.
Jiang, M., He, G., Li, J., Li, J., Guo, X., Gao, J., 2021. Hypoxic exposure activates the B cell-specific Moloney murine leukaemia virus integration site 1/PI3K/Akt axis and promotes EMT in leukaemia stem cells. Oncol. Lett. 21, 98.
Kahlert, U.D., Joseph, J.V., Kruyt, F.A.E., 2017. EMT- and MET-related processes in nonepithelial tumors: importance for disease progression, prognosis, and therapeutic opportunities. Mol. Oncol. 11, 860–877.
Kumagai, K., Nimura, Y., Mizota, A., Miyahara, N., Aoki, M., Furusawa, Y., Takiguchi, M., Yamamoto, S., Seki, N., 2006. Arpc1b gene is a candidate prediction marker for choroidal malignant melanomas sensitive to radiotherapy. Invest. Ophthalmol. Vis. Sci. 47, 2300–2304.
Kurisu, S., Takenawa, T., 2010. WASP and WAVE family proteins: friends or foes in cancer invasion? Cancer Sci. 101, 2093–2104.
Laurila, E., Savinainen, K., Kuuselo, R., Karhu, R., Kallioniemi, A., 2009. Characterization of the 7q21-q22 amplicon identifies ARPC1A, a subunit of the Arp2/3 complex, as a regulator of cell migration and invasion in pancreatic cancer. Genes Chromosomes Cancer 48, 330–339.
Lavenus, S.B., Tudor, S.M., Ullo, M.F., Vosatka, K.W., Logue, J.S., 2020. A flexible network of vimentin intermediate filaments promotes migration of amoeboid cancer cells through confined environments. J. Biol. Chem. 295, 6700–6709.
Leung, G., Zhou, Y., Ostrowski, P., Mylvaganam, S., Boroumand, P., Mulder, D.J., Guo, C., Muise, A.M., Freeman, S.A., 2021. ARPC1B binds WASP to control actin polymerization and curtail tonic signaling in B cells. JCI Insight 6.
Li, Y., Dai, C., Wu, C., Liu, Y., 2007. PINCH-1 promotes tubular epithelial-to-mesenchymal transition by interacting with integrin-linked kinase. J. Am. Soc. Nephrol.: JASN 18, 2534–2543.
Ligorio, M., Sil, S., Malagon-Lopez, J., Nieman, L.T., Misale, S., Di Pilato, M., Ebright, R. Y., Karabacak, M.N., Kulkarni, A.S., Liu, A., Vincent Jordan, N., Franses, J.W., Philipp, J., Kreuzer, J., Desai, N., Arora, K.S., Rajurkar, M., Horwitz, E., Neyaz, A., Tai, E., Magnus, N.K.C., Vo, K.D., Yashaswini, C.N., Marangoni, F., Boukhali, M., Fatherree, J.P., Damon, L.J., Xega, K., Desai, R., Choz, M., Bersani, F., Langenbucher, A., Thapar, V., Morris, R., Wellner, U.F., Schilling, O., Lawrence, M. S., Liss, A.S., Rivera, M.N., Deshpande, V., Benes, C.H., Maheswaran, S., Haber, D.A., Fernandez-Del-Castillo, C., Ferrone, C.R., Haas, W., Aryee, M.J., Ting, D.T., 2019. Stromal microenvironment shapes the intratumoral architecture of pancreatic cancer. Cell 178, 160–175 e127.
Lin, C.W., Wang, L.K., Wang, S.P., Chang, Y.L., Wu, Y.Y., Chen, H.Y., Hsiao, T.H., Lai, W. Y., Lu, H.H., Chang, Y.H., Yang, S.C., Lin, M.W., Chen, C.Y., Hong, T.M., Yang, P.C., 2016. Daxx inhibits hypoxia-induced lung cancer cell metastasis by suppressing the HIF-1alpha/HDAC1/Slug axis. Nat. Commun. 7, 13867.
Linder, S., Cervero, P., Eddy, R., Condeelis, J., 2023. Mechanisms and roles of podosomes and invadopodia. Nat. Rev. Mol. Cell Biol. 24, 86–106.
Liu, J., Lichtenberg, T., Hoadley, K.A., Poisson, L.M., Lazar, A.J., Cherniack, A.D., Kovatich, A.J., Benz, C.C., Levine, D.A., Lee, A.V., Omberg, L., Wolf, D.M., Shriver, C. D., Thorsson, V., , N. Cancer Genome Atlas Research, Hu, H., 2018. An integrated TCGA pan-cancer clinical data resource to drive high-quality survival outcome analytics. Cell 173, 400–416 e411.
Liu, T., Zhu, C., Chen, X., Wu, J., Guan, G., Zou, C., Shen, S., Chen, L., Cheng, P., Cheng, W., Wu, A., 2022. Dual role of ARPC1B in regulating the network between tumor-associated macrophages and tumor cells in glioblastoma. Oncoimmunology 11, 2031499.
Malagoli Tagliazucchi, G., Wiecek, A.J., Withnell, E., Secrier, M., 2023. Genomic and microenvironmental heterogeneity shaping epithelial-to-mesenchymal trajectories in cancer. Nat. Commun. 14, 789.
Marjon, K.D., Termini, C.M., Karlen, K.L., Saito-Reis, C., Soria, C.E., Lidke, K.A., Gillette, J.M., 2016. Tetraspanin CD82 regulates bone marrow homing of acute myeloid leukemia by modulating the molecular organization of N-cadherin. Oncogene 35, 4132–4140.
McDonald, P.C., Dedhar, S., 2022. New perspectives on the role of integrin-linked kinase (ILK) signaling in cancer metastasis. Cancers (Basel) 14.
Meng, J., Chen, S., Han, J.X., Qian, B., Wang, X.R., Zhong, W.L., Qin, Y., Zhang, H., Gao, W.F., Lei, Y.Y., Yang, W., Yang, L., Zhang, C., Liu, H.J., Liu, Y.R., Zhou, H.G., Sun, T., Yang, C., 2018. Twist1 regulates vimentin through Cul2 circular RNA to promote EMT in hepatocellular carcinoma. Cancer Res. 78, 4150–4162.
Menotti, M., Ambrogio, C., Cheong, T.C., Pighi, C., Mota, I., Cassel, S.H., Compagno, M., Wang, Q., Dall'Olio, R., Minero, V.G., Poggio, T., Sharma, G.G., Patrucco, E., Mastini, C., Choudhari, R., Pich, A., Zamo, A., Piva, R., Giliani, S., Mologni, L., Collings, C.K., Kadoch, C., Gambacorti-Passerini, C., Notarangelo, L.D., Anton, I.M., Voena, C., Chiarle, R., 2019. Wiskott-Aldrich syndrome protein (WASP) is a tumor suppressor in T cell lymphoma. Nat. Med. 25, 130–140.
Noman, M.Z., Janji, B., Abdou, A., Hasmim, M., Terry, S., Tan, T.Z., Mami-Chouaib, F., Thiery, J.P., Chouaib, S., 2017. The immune checkpoint ligand PD-L1 is upregulated in EMT-activated human breast cancer cells by a mechanism involving ZEB-1 and miR-200. Oncoimmunology 6, e1263412.
Pastushenko, I., Blanpain, C., 2019. EMT transition states during tumor progression and metastasis. Trends Cell Biol. 29, 212–226.
Pastushenko, I., Brisebarre, A., Sifrim, A., Fioramonti, M., Revenco, T., Boumahdi, S., Van Keymeulen, A., Brown, D., Moers, V., Lemaire, S., De Clercq, S., Minguijon, E., Balsat, C., Sokolow, Y., Dubois, C., De Cock, F., Scozzaro, S., Sopena, F., Lanas, A., D'Haene, N., Salmon, I., Marine, J.C., Voet, T., Sotiropoulou, P.A., Blanpain, C., 2018. Identification of the tumour transition states occurring during EMT. Nature 556, 463–468.
Percio, S., Coltella, N., Grisanti, S., Bernardi, R., Pattini, L., 2014. A HIF-1 network reveals characteristics of epithelial-mesenchymal transition in acute promyelocytic leukemia. Genome Med. 6, 84.
Pereira, W.O., De Carvalho, D.D., Zenteno, M.E., Ribeiro, B.F., Jacysyn, J.F., Sardinha, L. R., Zanichelli, M.A., Hamerschlak, N., Jones, G.E., Pagnano, K.B., Castro, F.A., Calle, Y., Amarante-Mendes, G.P., 2017. BCR-ABL1-induced downregulation of WASP in chronic myeloid leukemia involves epigenetic modification and contributes to malignancy. Cell death Dis. 8, e3114.
Pirillo, C., Birch, F., Tissot, F.S., Anton, S.G., Haltalli, M., Tini, V., Kong, I., Piot, C., Partridge, B., Pospori, C., Keeshan, K., Santamaria, S., Hawkins, E., Falini, B., Marra, A., Duarte, D., Lee, C.F., Roberts, E., Lo Celso, C., 2022. Metalloproteinase inhibition reduces AML growth, prevents stem cell loss, and improves chemotherapy effectiveness. Blood Adv. 6, 3126–3141.
Qu, S., Huang, X., Guo, X., Zheng, Z., Wei, T., Chen, B., 2023. Metastasis related epithelial-mesenchymal transition signature predicts prognosis and response to chemotherapy in acute myeloid leukemia. Drug Des. Devel Ther. 17, 1651–1663.
Ramundo, V., Giribaldi, G., Aldieri, E., 2021. Transforming growth factor-beta and oxidative stress in cancer: A crosstalk in driving tumor transformation. Cancers (Basel) 13.
Rauhala, H.E., Teppo, S., Niemela, S., Kallioniemi, A., 2013. Silencing of the ARP2/3 complex disturbs pancreatic cancer cell migration. Anticancer Res. 33, 45–52.
Robinson, D., Van Allen, E.M., Wu, Y.M., Schultz, N., Lonigro, R.J., Mosquera, J.M., Montgomery, B., Taplin, M.E., Pritchard, C.C., Attard, G., Beltran, H., Abida, W., Bradley, R.K., Vinson, J., Cao, X., Vats, P., Kunju, L.P., Hussain, M., Feng, F.Y., Tomlins, S.A., Cooney, K.A., Smith, D.C., Brennan, C., Siddiqui, J., Mehra, R., Chen, Y., Rathkopf, D.E., Morris, M.J., Solomon, S.B., Durack, J.C., Reuter, V.E., Gopalan, A., Gao, J., Loda, M., Lis, R.T., Bowden, M., Balk, S.P., Gaviola, G., Sougnez, C., Gupta, M., Yu, E.Y., Mostaghel, E.A., Cheng, H.H., Mulcahy, H., True, L. D., Plymate, S.R., Dvinge, H., Ferraldeschi, R., Flohr, P., Miranda, S., Zafeiriou, Z., Tunariu, N., Mateo, J., Perez-Lopez, R., Demichelis, F., Robinson, B.D., Schiffman, M., Nanus, D.M., Tagawa, S.T., Sigaras, A., Eng, K.W., Elemento, O., Sboner, A., Heath, E.I., Scher, H.I., Pienta, K.J., Kantoff, P., de Bono, J.S., Rubin, M. A., Nelson, P.S., Garraway, L.A., Sawyers, C.L., Chinnaiyan, A.M., 2015. Integrative clinical genomics of advanced prostate cancer. Cell 161, 1215–1228.
Salvi, A., Thanabalu, T., 2017. WIP promotes in-vitro invasion ability, anchorage independent growth and EMT progression of A549 lung adenocarcinoma cells by regulating RhoA levels. Biochem Biophys. Res. Commun. 482, 1353–1359.

Sawicki, G., Matsuzaki, A., Janowska-Wieczorek, A., 1998. Expression of the active form of MMP-2 on the surface of leukemic cells accounts for their in vitro invasion. J. Cancer Res. Clin. Oncol. 124, 245–252.
Schrank, B.R., Aparicio, T., Li, Y., Chang, W., Chait, B.T., Gundersen, G.G., Gottesman, M.E., Gautier, J., 2018. Nuclear ARP2/3 drives DNA break clustering for homology-directed repair. Nature 559, 61–66.
Shaebani, M.R., Stankevicins, L., Vesperini, D., Urbanska, M., Flormann, D.A.D., Terriac, E., Gad, A.K.B., Cheng, F., Eriksson, J.E., Lautenschlager, F., 2022. Effects of vimentin on the migration, search efficiency, and mechanical resilience of dendritic cells. Biophys. J. 121, 3950–3961.
Snyder, A., Makarov, V., Merghoub, T., Yuan, J., Zaretsky, J.M., Desrichard, A., Walsh, L. A., Postow, M.A., Wong, P., Ho, T.S., Hollmann, T.J., Bruggeman, C., Kannan, K., Li, Y., Elipenahli, C., Liu, C., Harbison, C.T., Wang, L., Ribas, A., Wolchok, J.D., Chan, T.A., 2014. Genetic basis for clinical response to CTLA-4 blockade in melanoma. N. Engl. J. Med. 371, 2189–2199.
Song, J.H., Kim, S.H., Cho, D., Lee, I.K., Kim, H.J., Kim, T.S., 2009. Enhanced invasiveness of drug-resistant acute myeloid leukemia cells through increased expression of matrix metalloproteinase-2. Int. J. Cancer 125, 1074–1081.
Stavropoulou, V., Kaspar, S., Brault, L., Sanders, M.A., Juge, S., Morettini, S., Tzankov, A., Iacovino, M., Lau, I.J., Milne, T.A., Royo, H., Kyba, M., Valk, P.J., Peters, A.H., Schwaller, J., 2016. MLL-AF9 expression in hematopoietic stem cells drives a highly invasive AML expressing EMT-related genes linked to poor outcome. Cancer Cell 30, 43–58.
Tavor, S., Petit, I., Porozov, S., Goichberg, P., Avigdor, A., Sagiv, S., Nagler, A., Naparstek, E., Lapidot, T., 2005. Motility, proliferation, and egress to the circulation of human AML cells are elastase dependent in NOD/SCID chimeric mice. Blood 106, 2120–2127.
Terry, S., Savagner, P., Ortiz-Cuaran, S., Mahjoubi, L., Saintigny, P., Thiery, J.P., Chouaib, S., 2017. New insights into the role of EMT in tumor immune escape. Mol. Oncol. 11, 824–846.
Thiery, J.P., Sleeman, J.P., 2006. Complex networks orchestrate epithelial-mesenchymal transitions. Nat. Rev. Mol. Cell Biol. 7, 131–142.
Tyner, J.W., Tognon, C.E., Bottomly, D., Wilmot, B., Kurtz, S.E., Savage, S.L., Long, N., Schultz, A.R., Traer, E., Abel, M., Agarwal, A., Blucher, A., Borate, U., Bryant, J., Burke, R., Carlos, A., Carpenter, R., Carroll, J., Chang, B.H., Coblentz, C., d'Almeida, A., Cook, R., Danilov, A., Dao, K.T., Degnin, M., Devine, D., Dibb, J., Edwards, D.Kt, Eide, C.A., English, I., Glover, J., Henson, R., Ho, H., Jemal, A., Johnson, K., Johnson, R., Junio, B., Kaempf, A., Leonard, J., Lin, C., Liu, S.Q., Lo, P., Loriaux, M.M., Luty, S., Macey, T., MacManiman, J., Martinez, J., Mori, M., Nelson, D., Nichols, C., Peters, J., Ramsdill, J., Rofelty, A., Schuff, R., Searles, R., Segerdell, E., Smith, R.L., Spurgeon, S.E., Sweeney, T., Thapa, A., Visser, C., Wagner, J., Watanabe-Smith, K., Werth, K., Wolf, J., White, L., Yates, A., Zhang, H., Cogle, C.R., Collins, R.H., Connolly, D.C., Deininger, M.W., Drusbosky, L., Hourigan, C.S., Jordan, C.T., Kropf, P., Lin, T.L., Martinez, M.E., Medeiros, B.C., Pallapati, R.R., Pollyea, D.A., Swords, R.T., Watts, J.M., Weir, S.J., Wiest, D.L., Winters, R.M., McWeeney, S.K., Druker, B.J., 2018. Functional genomic landscape of acute myeloid leukaemia. Nature 562, 526–531.
von Loeffelholz, O., Purkiss, A., Cao, L., Kjaer, S., Kogata, N., Romet-Lemonne, G., Way, M., Moores, C.A., 2020. Cryo-EM of human Arp2/3 complexes provides structural insights into actin nucleation modulation by ARPC5 isoforms. Biol. Open 9.
Wang, C., Sample, K.M., Gajendran, B., Kapranov, P., Liu, W., Hu, A., Zacksenhaus, E., Li, Y., Hao, X., Ben-David, Y., 2021. FLI1 induces megakaryopoiesis gene expression through WAS/WIP-dependent and independent mechanisms; implications for wiskott-aldrich syndrome. Front Immunol. 12, 607836.
Wang, L., Zhang, F., Cui, J.Y., Chen, L., Chen, Y.T., Liu, B.W., 2018. CAFs enhance paclitaxel resistance by inducing EMT through the IL-6/JAK2/STAT3 pathway. Oncol. Rep. 39, 2081–2090.
Wang, R., Khan, S., Liao, G., Wu, Y., Tang, D.D., 2022. Nestin modulates airway smooth muscle cell migration by affecting spatial rearrangement of vimentin network and focal adhesion assembly. Cells 11.
Whiteley, A.E., Price, T.T., Cantelli, G., Sipkins, D.A., 2021. Leukaemia: a model metastatic disease. Nat. Rev. Cancer 21, 461–475.
Wu, S., Du, Y., Beckford, J., Alachkar, H., 2018. Upregulation of the EMT marker vimentin is associated with poor clinical outcome in acute myeloid leukemia. J. Transl. Med 16, 170.
Xu, Q., Zhang, Q., Dong, M., Yu, Y., 2021. MicroRNA-638 inhibits the progression of breast cancer through targeting HOXA9 and suppressing Wnt/beta-cadherin pathway. World J. Surg. Oncol. 19, 247.
Yang, J., Antin, P., Berx, G., Blanpain, C., Brabletz, T., Bronner, M., Campbell, K., Cano, A., Casanova, J., Christofori, G., Dedhar, S., Derynck, R., Ford, H.L., Fuxe, J., Garcia de Herreros, A., Goodall, G.J., Hadjantonakis, A.K., Huang, R.J.Y., Kalcheim, C., Kalluri, R., Kang, Y., Khew-Goodall, Y., Levine, H., Liu, J., Longmore, G.D., Mani, S.A., Massague, J., Mayor, R., McClay, D., Mostov, K.E., Newgreen, D.F., Nieto, M.A., Puisieux, A., Runyan, R., Savagner, P., Stanger, B., Stemmler, M.P., Takahashi, Y., Takeichi, M., Theveneau, E., Thiery, J.P., Thompson, E.W., Weinberg, R.A., Williams, E.D., Xing, J., Zhou, B.P., Sheng, G., Association, E.M.T.I., 2020. Guidelines and definitions for research on epithelial-mesenchymal transition. Nat. Rev. Mol. Cell Biol. 21, 341–352.
Yu, X., Wang, Q., Liu, B., Zhang, N., Cheng, G., 2021. Vitamin D enhances radiosensitivity of colorectal cancer by reversing epithelial-mesenchymal transition. Front Cell Dev. Biol. 9, 684855.
Zhang, B., Wu, K.F., Cao, Z.Y., Rao, Q., Ma, X.T., Zheng, G.G., Li, G., 2004. IL-18 increases invasiveness of HL-60 myeloid leukemia cells: up-regulation of matrix metalloproteinases-9 (MMP-9) expression. Leuk. Res. 28, 91–95.
Zhang, B., Li, Y., Wu, Q., Xie, L., Barwick, B., Fu, C., Li, X., Wu, D., Xia, S., Chen, J., Qian, W.P., Yang, L., Osunkoya, A.O., Boise, L., Vertino, P.M., Zhao, Y., Li, M., Chen, H.R., Kowalski, J., Kucuk, O., Zhou, W., Dong, J.T., 2021a. Acetylation of KLF5 maintains EMT and tumorigenicity to cause chemoresistant bone metastasis in prostate cancer. Nat. Commun. 12, 1714.
Zhang, N., Ng, A.S., Cai, S., Li, Q., Yang, L., Kerr, D., 2021b. Novel therapeutic strategies: targeting epithelial-mesenchymal transition in colorectal cancer. Lancet Oncol. 22, e358–e368.
Zhang, T.J., Zhou, J.D., Ma, J.C., Deng, Z.Q., Qian, Z., Yao, D.M., Yang, J., Li, X.X., Lin, J., Qian, J., 2017. CDH1 (E-cadherin) expression independently affects clinical outcome in acute myeloid leukemia with normal cytogenetics. Clin. Chem. Lab. Med. 55, 123–131.
Zhang, W., Xing, L., Xu, L., Jin, X., Du, Y., Feng, X., Liu, S., Liu, Q., 2019. Nudel involvement in the high-glucose-induced epithelial-mesenchymal transition of tubular epithelial cells. Am. J. Physiol. Ren. Physiol. 316, F186–F194.
Zhang, Y., Zeng, S., Ma, J., Deng, G., Qu, Y., Guo, C., Shen, H., 2016. Nestin overexpression in hepatocellular carcinoma associates with epithelial-mesenchymal transition and chemoresistance. J. Exp. Clin. Cancer Res. 35, 111.
Zhang, Z., Li, L., Wu, C., Yin, G., Zhu, P., Zhou, Y., Hong, Y., Ni, H., Qian, Z., Wu, W.S., 2020. Inhibition of Slug effectively targets leukemia stem cells via the Slc13a3/ROS signaling pathway. Leukemia 34, 380–390.